
FETA: Towards Specializing Foundation Models for Expert Task Applications

Amit Alfassy*^{1,3} Assaf Arbelle*¹ Oshri Halimi^{1,3} Sivan Harary¹
Roi Herzig¹ Eli Schwartz¹ Rameswar Panda¹ Michele Dolfi¹
Christoph Auer¹ Kate Saenko^{2,4} Peter W. J. Staar¹ Rogerio Feris² Leonid Karlinsky*²

¹IBM Research, ²MIT-IBM AI-Watson Lab, ³Technion, ⁴Boston University

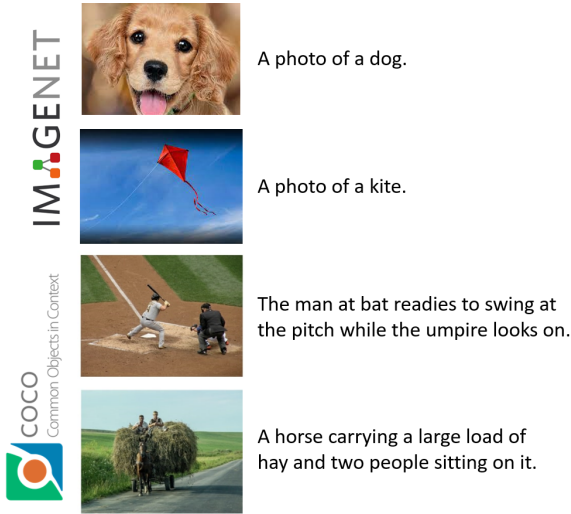
Abstract

Foundation Models (FMs) have demonstrated unprecedented capabilities including zero-shot learning, high fidelity data synthesis, and out of domain generalization. However, as we show in this paper, FMs still have poor out-of-the-box performance on expert tasks (e.g. retrieval of car manuals technical illustrations from language queries), data for which is either unseen or belonging to a long-tail part of the data distribution of the huge datasets used for FM pre-training. This underlines the necessity to explicitly evaluate and finetune FMs on such expert tasks, arguably ones that appear the most in practical real-world applications. In this paper, we propose a first of its kind FETA benchmark built around the task of teaching FMs to understand technical documentation, via learning to match their graphical illustrations to corresponding language descriptions. Our FETA benchmark focuses on text-to-image and image-to-text retrieval in public car manuals and sales catalogue brochures. FETA is equipped with a procedure for completely automatic annotation extraction (code would be released upon acceptance), allowing easy extension of FETA to more documentation types and application domains in the future. Our automatic annotation leads to an automated performance metric shown to be consistent with metrics computed on human-curated annotations (also released). We provide multiple baselines and analysis of popular FMs on FETA leading to several interesting findings that we believe would be very valuable to the FM community, paving the way towards real-world application of FMs for practical expert tasks currently “overlooked” by standard benchmarks focusing on common objects.

1 Introduction

Foundation Models (FMs) is a broad term, relating to models that through their training on huge data acquire “skills” going beyond the base training objectives [6]. They are commonly trained using hundreds of millions of data points and a collection of base tasks either uni-modal, e.g. only language, or multi-modal, e.g. text-image pairs. Remarkably, the skills acquired by FMs demonstrate very good transferability to a wide variety of new downstream tasks, many times with very limited or no data for the target task. Since their introduction in the Natural Language Processing (NLP) domain [6, 13, 47], FMs have been applied to uni-modal [8, 13, 47] and multi-modal [1, 15, 22, 31, 32, 33, 46, 53, 61, 64, 65] Vision & Language (V&L) scenarios, as well as demonstrated unprecedented capabilities for high fidelity data synthesis [41, 48, 50] and out of domain generalization [49]. However, despite the tremendous progress in FMs many gaps still remain open with regards to reaching human level performance in some mundane tasks [57], as well as in many human expert ones. In particular, for many types of ‘specialized’ data (e.g. illustrated technical, scientific documentation, medical, or other expert domains data), which are of the utmost interest for many real-world applications, FM performance is still lacking in many respects due to: (i) specialized

Common Objects Vision & Language Task Data



FETA Expert Task data



Figure 1: We introduce FETA, a novel dataset and benchmark for evaluating and improving Foundation (V&L) Models performance on expert data tasks. In contrast to mainstream benchmarks used to evaluate FMs, FETA does not focus on common objects captured with consumer cameras (left), instead providing a completely automatic pipeline for extracting (mostly other visual domains) expert data from publicly available technical and other documentation. Also, as opposed to original CLIP, FETA’s MIL-CLIP method can learn from multiple-hypothesis data automatically extracted from complex document’s pages (see right) comprised of multiple images and texts without apparent 1:1 association.

data may not be present in the web-crawled internet-scale datasets [17, 46, 51] used to train FMs; (ii) even if specialized data is present, it is deep in the long-tail of the data distribution statistics, meaning that due to the limited capacity, or the information bottleneck [58], of the FM models, useful representation features for this data are not significant in the FMs’ learned representation space; (iii) commonly, a large domain gap exists between natural image common-objects biased data and the accompanying text used for FM training and sketch-like / synthetic / non-consumer-camera imagery commonly appearing in expert data scenarios. This suggests that to be utilized for expert data applications, FMs need to be tuned to better represent this data, driving the under-represented features that are necessary for such data to emerge. But how can one analyze and tune for such effects?

Our proposed Foundation models for Expert Task Applications (FETA) benchmark and dataset is intended to bridging the gap between the ‘common object’ oriented benchmarks (e.g. ImageNet) currently used to evaluate V&L FM performance and more complex specialized objects (e.g. an engine diagram, or a car mechanical part) typical to many real-world applications targeting expert tasks. To the best of our knowledge, the FETA is the first benchmark aiming at evaluating and improving the FMs performance in the expert data domains. The first version of FETA focuses on Text-to-Image (T2I) & Image-to-Text (I2T) retrieval in technical documentation, specifically diverse car service manuals from multiple manufacturers, and sales (currently IKEA annual) catalogues. Our proposed automatic annotation process is general and can support ingestion of any variety of programmatic PDF documents with illustrations ¹, making FETA easily extensible to additional expert tasks and content domains, either by us (in future versions of FETA) or by other members of the community. The FETA is also equipped with our proposed method for automatic extraction of text-image pairs both for fine-tuning the models as well as for automatic performance evaluation. Our method is based on establishing multiple-hypothesis text-image correspondence via co-location of images and surrounding text on the pages of the processed PDFs. Although completely non-curated, we

¹our code for automatic ingestion and generating V&L text-image pairs supervision for arbitrary collection of programmatic PDFs with illustrations will be released upon acceptance

show how comparative metrics established by our proposed automatic annotation technique translate consistently to a metric established via manually curated ground truth data, thus indicating the utility of the proposed automatic metric which, as explained above, effortlessly extends to any arbitrary expert tasks and content domains we expect to be added to FETA in the future. Finally, we provide a large set of interesting baselines on our collected FETA data including popular off-the-shelf FMs, various methods for finetuning FMs on the train set of FETA, as well as some interesting application of a combination of Locked and Multiple-Instance-Learning fine-tuning schemes demonstrating significantly superior performance on both automatic as well as manually curated metrics of FETA, paving the way to real practical applications of the proposed fine-tuning techniques.

To summarize, our key contributions are as follows: (i) We propose *Foundation models for Expert Task Applications* (FETA) - first of its kind dataset and benchmark - targeting the evaluation and improvement of the Foundation Models performance on expert data domain tasks prevalent in real-world applications; (ii) We propose and release an automatic text-image pairs extraction pipeline fitting any collection of illustrated programmatic PDFs or even broader documents data, making our proposed FETA easily extensible to new content domains and expert data applications drawing from this abundant source of *expert* V&L data; (iii) We propose an automatic evaluation metric for FMs on expert tasks using our proposed data extraction pipeline and show this metric leads to consistent performance results relatively to the ones resulting from a manually curated metric (also released in FETA) (iv) We provide a large collection of baselines on FETA including out-of-the-box FMs, FETA tuned-FMs, and a novel combination of Low Ranked Adaptor finetuning using Multiple Instance Learning schemes reaching the best performance by a large margin; (v) Our findings corroborate our proposition that out-of-the-box FMs performance drops significantly when moving away from common object benchmarks and entering expert domains, underlining the value of our proposed FETA benchmark for future research towards paving the way to real-world practical applications of FMs in expert domains. The FETA dataset is available for download here².

2 Dataset Collection

2.1 Source and Description

Documents are a natural data-source to find text-image pairs, since images in documents have either captions or at the minimum are related to their surrounding textual content. In order to obtain real-world images, and not schematics or scientific figures, we chose documents related to consumer goods such as product catalogues and manuals. Such documents typically provide both images of the product and a textual description. This specific data was chosen due to several important criteria. First, the data is abundant with a large variety of text and images. Second, the data includes images which are not "natural" domain and belong to the long-tail distribution of the training data for the FMs. Finally, when collecting the data we considered the legal and privacy issues such that the data is freely available without any legal claims limiting its distribution. We downloaded 349 car service manuals from <https://www.workshopservicemanual.com/> each comprising 20 to 1602 pages. The documents were then processed, such that all text and images were automatically extracted. In the following sections we will describe in detail the automatic processing and annotation flow. Additionally, FETA also includes IKEA yearly catalogues data. The data was published by [69] for semantic based sentence recognition in images, the data is available for download³. The IKEA data was processed identically to the car-manuals dataset and is detailed in the supplementary material.

2.2 Data Conversion

The product-related source documents are in PDF format, which is notoriously hard to extract data from. In the past years, tools⁴ and cloud-services⁵ have been developed to convert PDF documents [3, 55] to JSON semantically, meaning that structural elements of the document (e.g. title, paragraphs, section-headers, tables, images, etc) are extracted semantically and easily accessible in the final JSON document. This semantic conversion is achieved by leveraging pre-trained ML methods for Layout-Segmentation [34, 43] & Table-Understanding [40]. In the Layout-Segmentation, document components such as text-blocks, tables and images are visually identified using state-of-

²<https://ai-vision-public-datasets.s3.eu.cloud-object-storage.appdomain.cloud/FETA/feta.tar.gz>

³<https://github.com/ivc-yz/SSR>

⁴<https://github.com/DS4SD/deepsearch-toolkit>

⁵<https://deepsearch-experience.res.ibm.com>

Table 1: **Dataset Statistics**. In total, the first version of FETA contains around 56K extracted images and around 89K pieces of extracted image related text. Additional statistics are available in Section 2 of the supplementary material.

| Manufacturer | Docs | Avg. Pages/Doc | Avg. Images/Doc | Avg. Texts/Doc |
|------------------|------|----------------|-----------------|----------------|
| Nissan | 275 | 149 | 138 | 249 |
| Toyota | 24 | 107 | 122 | 180 |
| Mazda | 9 | 149 | 413 | 657 |
| Chevrolet | 31 | 169 | 92 | 128 |
| Renault | 10 | 169 | 385 | 596 |
| Entire data Avg. | 349 | 149 | 147 | 254 |

the-art object-detection algorithms, which provide bounding-boxes for structural elements on each page. The latter allows us to geometrically link images to text via a heuristic geometric closeness relationship. The output JSON undergoes extended post processing, aiming to reduce parsing noise. For example: merge spatially close texts by finding connected components in a graph made by the texts. More information available in Section 1 of the supplementary material.

2.3 Automatic Annotation

In the spirit of Multiple Instance Learning (MIL), we defined the automatic matching of each extracted image with a set of up to five pieces of texts from the **same page**. Every image was paired with the most probable text block from the left, right, top, and bottom of the figure, when available. We also selected a text box if it was overlapping with the image. We found that in the majority of the cases, at least one of these blocks of text is related to the image. This inherently creates the many-to-many MIL scenario where each image is associated with multiple text instances and vice-versa. We further found that in some cases, an image can appear in several places within the document. Since our automatic annotation is based on the co-location of the image and text within the same page, these cases can hurt retrieval metrics when disregarded. We thus applied a filtering process to merge all occurrences of the same image within a single document (see Section 1.2 of the supplementary material).

2.4 Manual Annotation

Since both training and test data were automatically annotated, we chose to manually annotate a small subset of the data in order to validate the results. For this manually annotated set we randomly selected 15 documents and manually paired a single image with a single text within every page of each document. The manual annotation was done using the annotation tool of the DeepSearch cloud service, based on the automatic extraction of images and texts. As can be seen from Table 2 and Table 3, the results on the automatic and manual annotated set are highly correlated, thus strengthening the validity of our proposed automatic annotation for testing, and underlining the scalability of our approach in terms of adding data and future inclusion of additional expert domains.

2.5 Statistics

The **Car-Manuals** dataset consists of a total of 349 PDF documents from 5 car manufacturers, namely Nissan, Toyota, Mazda, Renault, Chevrolet. Table 1 details the statistics of the dataset by manufacturer. The **IKEA-catalogues** dataset contains 26 documents with 7366 pages total, approximately 9574 images and 23927 texts automatically extracted from those pages. More details on the IKEA-catalogues dataset, as well as analysis of the performance of our rich set of baselines on that dataset and further data statistics is provided in Section 2 of the supplementary material.

3 Baselines

3.1 Background

Our main out-of-the-box FM baseline is the most widely used and readily available V&L FM, CLIP [46]. CLIP was trained using a contrastive loss applied to the similarity of the textual and visual features of all image-text pairs within each batch. This simple yet effective method has proven to work fantastically on natural images when supplied with a huge amount (400M) of image-text pairs collected from the Web. However, as we show in our experiments (Table 2), CLIP’s performance on the document data based expert task is far from sufficient. This underlines the need to fine-tune models such as CLIP on expert tasks in order to adapt the model to practical use in expert applications.

But what is the best and most scalable way to fine-tune in this case? In the case of the automatic document data annotation, where there are no image-text pairs but rather sets of text associated to each image and sets of images associated with each text, we argue that the original contrastive loss can not be used, and the proposed MIL variants, inspired by [38] from the video domain, should be used instead. Additionally, expert data is quite diverse and significantly small compared to the tremendous volumes of pre-training data used to make CLIP. We therefore also explore different constrained fine-tuning strategies based on encoder-locking ideas from [66].

CLIP. The CLIP model is comprised of an image encoder and a text encoder. Let \mathcal{M}_I and \mathcal{M}_T be the image and text encoders respectively. For a given image I_i , and a piece of text T_i , we define the image and the text embedding vectors as the outputs of \mathcal{M}_I and \mathcal{M}_T , respectively:

$$x_i = \mathcal{M}_I(I_i), \quad y_i = \mathcal{M}_T(T_i) \quad (1)$$

Standard supervised learning assumes that the samples and targets are paired, $\{x_i, y_i\}_{i=1}^N$, where N is the size of the dataset. For a given batch of samples, B , the standard CLIP loss is a cross-entropy loss defined as:

$$\mathcal{L}_{CLIP} = -\frac{1}{2B} \left(\sum_i^B \log \frac{\exp(x_i^T y_i / \sigma)}{\sum_{j=1}^B \exp(x_i^T y_j / \sigma)} + \sum_i^B \log \frac{\exp(y_i^T x_i / \sigma)}{\sum_{j=1}^B \exp(y_i^T x_j / \sigma)} \right) \quad (2)$$

where σ is a normalization factor, often set as a learned parameter.

We propose an extension to the CLIP contrastive loss, adapting it to a MIL setting where we know that at least one of the texts is a positive match to the image and vice versa.

3.2 MIL-CLIP

The MIL setting, relaxes the paired assumption and defines a "bag" of M targets $\{y_i^m\}_{m=0}^M$ such that at least one of the targets (e.g. texts) is a positive match to the sample (e.g. image). This weak annotation aligns perfectly with our automatic annotation framework.

There are several ways to modify the original loss (Eq. 2) to the MIL setting. Next, we will present a few plausible baselines.

MIL-Max. A simple yet effective method for MIL is by selecting the positive example as the maximum value over the bag of labels. Defining $\hat{m}_i = \arg \max_m x_i^T y_i^m$:

$$\begin{aligned} \mathcal{L}_{MAX} = & -\frac{1}{B} \sum_i^B \log \frac{\exp(x_i^T y_i^{\hat{m}_i} / \sigma)}{\exp(x_i^T y_i^{\hat{m}_i} / \sigma) + \sum_{j \neq i}^B \sum_m \exp(x_i^T y_j^m / \sigma)} \\ & -\frac{1}{B} \sum_i^B \max_q \log \frac{\exp((y_i^q)^T x_i / \sigma)}{\exp(y_i^{qT} x_i / \sigma) + \sum_{j \neq i}^B \sum_m \exp(y_i^{mT} x_j / \sigma)} \end{aligned} \quad (3)$$

MIL-SoftMax. A small modification to the MIL-Max loss is replacing the maximum with a SoftMax weighted average of the nominator of the loss function. For convenience we first define the SoftMax weights with scaling factor σ_{sm} as:

$$S_i^m = \frac{\exp(x_i^T y_i^m / \sigma_{sm})}{\sum_{n=1}^M \exp(x_i^T y_i^n / \sigma_{sm})} \quad (4)$$

and define the MIL-SoftMax variant as:

$$\begin{aligned} \mathcal{L}_{SM} = & -\frac{1}{B} \sum_i^B \log \frac{\sum_m S_i^m \exp(x_i^T y_i^m / \sigma)}{\sum_m S_i^m \exp(x_i^T y_i^m / \sigma) + \sum_{j \neq i}^B \sum_m \exp(x_i^T y_j^m / \sigma)} \\ & -\frac{1}{B} \sum_i^B \max_q \log \frac{\exp(y_i^{qT} x_i / \sigma)}{\exp(y_i^{qT} x_i / \sigma) + \sum_{j \neq i}^B \sum_m \exp(y_i^{mT} x_j / \sigma)} \end{aligned} \quad (5)$$

MIL-NCE. Recently the MIL-NCE [38] approach was proposed for visual representation learning from uncurated videos. We adapt the MIL-NCE loss to fit the clip, contrastive loss as follows :

$$\mathcal{L}_{NCE} = -\frac{1}{B} \sum_i^B \log \frac{\sum_m \exp(x_i^T y_i^m / \sigma)}{\sum_{j=1}^B \sum_m \exp(x_i^T y_j^m / \sigma)} \quad (6)$$

Following the ablation study presented in the supplementary material, unless stated otherwise we chose the MIL-NCE version in all our experiments.

3.3 CLIP-LoRA

LoRA [18] proposed Low-Rank Adapters for large language models. LoRA locks the original weights of a pretrained model and adds trainable low rank residual adapters to different model layers. LoRA build upon the observation that in many cases learned layer weight matrices are in fact of low-rank, hence adapting them with a low-rank constraint on the change leads to good results also increasing efficiency and reducing over-fitting. We defer in our use of LoRA adapters both from the original work of [18], as well as from the only reported use of this tool for V&L models so far: [56]. As opposed to [18] and [56] that injected LoRA only into query/value projections of transformer MHSA blocks ([18]) or introduced them only to the text encoder ([56]), we found that also using LoRA weights in all nn.Conv2d, nn.Linear and nn.Embedding layers, results in significantly bigger performance gains. Additionally, we also apply LoRA outside just the transformer models - also to the CLIP ResNet50 backbone image encoder where applicable.

3.4 Implementation Details

We base our code on the open project [19] https://github.com/mlfoundations/open_clip. All our experiments used ResNet50 backbone models using the original CLIP [46] pre-trained models (400M image-text pairs). All fine-tuning experiments were run with 5e-05 learning rate, 64 batch size, and 20 epochs, using PyTorch DDP. We provide our code, including our automatic data annotation and all the baselines, in the supplementary and will release it upon acceptance. All the models were trained using either an Nvidia A100 or V100 GPU, with 8 GPUs per experiment.

4 Experiments

4.1 Data Splits

In all of the following experiments the data was split into five folds for each manufacturer and the results presented are an average over the results of the five-fold training and testing regime. The results are further averaged across manufacturers. Our folds are splitting on complete documents, not on document pages, so pages from the same document never appear in both train and test. We next present a detailed set of baseline experiments under four different settings: (i) *Many-Shot*: training on four folds of a *Nissan manufacturer*, as it contains the largest collection of documents, and testing on the remaining fifth fold; (ii) *Zero-Shot*: training on all data of all but one manufacturer, testing on all the data of the left-out manufacturer; . (iii) *One-shot*: similar to *Zero-Shot* but adding one document of the left-out manufacturer, testing on the remaining data of the left-out manufacturer, this is repeated five times with a different document each time; (iv) *Few-shot*: similar to *One-Shot* but adding one **fold** of the left-out manufacturer, testing on the remaining folds of the left-out manufacturer, this is repeated five times with a different document each time.

4.2 Baseline Methods

In addition to our MIL-CLIP method we evaluate three simple CLIP-based baselines: (i) *CLIP*: We test the pre-trained CLIP400M model without any further training. (ii) *Concatenate*: During training we concatenate all texts from the MIL "bag" into one long text and set it as the positive example and train using the original CLIP loss (Eq. 2). (iii) *Choose-One*: During training we randomly select one of the texts from the MIL "bag" as the positive example and train using the original CLIP loss (Eq. 2). For both *Concatenate* and *Choose-One* we test both Locked and non-Locked variants. Additional information on the evaluation of FLAVA [53], ALBEF [32], and ViLT [26] is available in Section 4.3 of the supplementary material.

4.3 Results

Table 2 presents the comparison of three baseline methods (also with or without Locking) under four different data split settings. These empirical results lead to several interesting conclusions. **First**, the CLIP model under-performs with respect to all the fine-tuning methods in the *Zero-Shot* and other settings, strengthening our hypothesis that FMs indeed need to be fine-tuned for expert domain (practical) applications such as explored in FETA, and their massive-scale pre-training is not sufficient for this tasks on its own. **Second**, fine-tuning using automatically collected V&L annotations induces significant performance improvements in many cases, especially in the *Many-Shot* case, which is arguably the most practical scenario, as the annotations are automatic hence the train data can scale

Table 2: **Main Results:** Image-to-Text and Text-to-Image retrieval accuracy for different baselines under three different data-split settings. Our baselines include out-of-the-box CLIP (additional FM results provided in Supplementary), several variants of its non-MIL and MIL fine-tuning variants. Our experimental settings include Many-Shot (train and test on same manufacturer data with lots of train samples), Zero-Shot (train and test on different manufacturers data), One-Shot (like Zero-Shot, but include a single document of the tested manufacturer in training), and Few-Shot (like Zero-Shot, but include a single fold of the tested manufacturer data in training). Results are averaged across manufacturers. All the experiments were performed on the automatically annotated data using five-folds and (naturally) without any overlap between train and test (on the level that pages of the same document *never appear* in both train and test). The "Locked" column refers to versions trained with locked (frozen) parameters of the image encoder \mathcal{M}_I . For reference, in FETA - the random chance probabilities for guessing the correct text match or the correct image match are 1.14% and 0.67% respectively. Numbers in **bold/blue** mark the best and second-best results, respectively.

| | Image-to-Text | | | | Text-to-Image | | | |
|-----------|---------------|--------|--------------|--------------|---------------|--------------|--------------|--------------|
| | Name | Locked | Rec@1 | Rec@5 | Rec@10 | Rec@1 | Rec@5 | Rec@10 |
| Zero-Shot | CLIP [46] | | 9.7% | 26.6% | 38.1% | 10.1% | 26.7% | 39.5% |
| | FLAVA [53] | | 4.0% | 16.6% | 29.7% | 5.5% | 19.8% | 34.5% |
| | ViT [26] | | 2.9% | 11.5% | 22.0% | 3.5% | 14.3% | 26.7% |
| | ALBEF [32] | | 3.9% | 16.6% | 26.7% | 4.4% | 18.4% | 31.2% |
| | Concatenate | | 6.5% | 20.4% | 31.5% | 7.1% | 25.0% | 38.4% |
| | Concatenate | ✓ | 9.4% | 25.0% | 36.7% | 8.1% | 24.0% | 37.6% |
| | Choose-One | | 10.7% | 27.6% | 39.9% | 9.3% | 28.1% | 41.8% |
| | Choose-One | ✓ | 10.40% | 26.7% | 39.3% | 9.20% | 25.6% | 37.9% |
| | CLIP-MIL | | 10.5% | 34.0% | 48.5% | 11.7% | 32.9% | 47.9% |
| | CLIP-MIL | ✓ | 11.0% | 29.2% | 40.0% | 9.7% | 28.1% | 40.6% |
| One-Shot | CLIP [46] | | 9.7% | 26.6% | 38.1% | 10.1% | 26.7% | 39.4% |
| | FLAVA [53] | | 4.0% | 16.6% | 29.7% | 5.5% | 19.8% | 34.5% |
| | ViT [26] | | 2.9% | 11.5% | 22.0% | 3.5% | 14.3% | 26.7% |
| | ALBEF [32] | | 3.9% | 16.6% | 26.7% | 4.4% | 18.4% | 31.2% |
| | Concatenate | | 10.3% | 27.3% | 39.2% | 9.5% | 27.0% | 40.8% |
| | Concatenate | ✓ | 8.7% | 24.4% | 37.0% | 7.9% | 25.1% | 38.5% |
| | Choose-One | | 10.3% | 27.2% | 39.5% | 9.4% | 27.5% | 41.6% |
| | Choose-One | ✓ | 10.4% | 28.0% | 39.9% | 8.9% | 25.5% | 37.9% |
| | CLIP-MIL | | 11.0% | 30.3% | 43.2% | 9.9% | 27.9% | 40.9% |
| | CLIP-MIL | ✓ | 11.9% | 30.3% | 42.5% | 10.9% | 29.4% | 43.2% |
| Few-Shot | CLIP [46] | | 8.6% | 25.6% | 37.2% | 9.2% | 24.3% | 36.6% |
| | FLAVA [53] | | 3.9% | 16.7% | 30.1% | 5.2% | 18.5% | 32.7% |
| | ViT [26] | | 2.8% | 11.1% | 21.6% | 3.2% | 13.3% | 25.4% |
| | ALBEF [32] | | 3.9% | 13.1% | 25.5% | 4.2% | 17.4% | 29.6% |
| | Concatenate | | 9.0% | 26.5% | 40.3% | 10.3% | 29.6% | 44.7% |
| | Concatenate | ✓ | 8.4% | 24.5% | 38.5% | 10.5% | 29.0% | 41.8% |
| | Choose-One | | 11.2% | 30.5% | 44.2% | 13.1% | 31.3% | 46.4% |
| | Choose-One | ✓ | 11.6% | 31.5% | 44.7% | 11.6% | 29.0% | 44.0% |
| | CLIP-MIL | | 14.1% | 36.7% | 48.9% | 15.0% | 35.2% | 50.0% |
| | CLIP-MIL | ✓ | 13.8% | 33.7% | 47.5% | 11.6% | 33.0% | 47.0% |
| Many-Shot | CLIP [46] | | 13.8% | 31.2% | 41.6% | 13.6% | 36.4% | 50.7% |
| | FLAVA [53] | | 4.2% | 16.1% | 27.8% | 6.6% | 24.4% | 41.0% |
| | ViT [26] | | 3.1% | 13.3% | 23.4% | 4.4% | 18.3% | 32.0% |
| | ALBEF [32] | | 3.8% | 15.8% | 26.6% | 5.5% | 22.4% | 37.5% |
| | Concatenate | | 18.4% | 37.8% | 49.9% | 15.9% | 42.1% | 58.3% |
| | Concatenate | ✓ | 20.7% | 39.7% | 51.3% | 16.2% | 41.2% | 56.2% |
| | Choose-One | | 24.5% | 49.9% | 62.2% | 21.2% | 52.3% | 67.2% |
| | Choose-One | ✓ | 27.7% | 52.7% | 64.1% | 21.6% | 52.1% | 66.5% |
| | CLIP-MIL | | 32.6% | 56.2% | 66.7% | 27.8% | 59.0% | 72.3% |
| | CLIP-MIL | ✓ | 34.5% | 56.8% | 66.1% | 27.2% | 57.9% | 70.7% |

Table 3: **Results on manually curated data:** Image-Text retrieval accuracy results. Models trained on automatically annotated data in the same way as in table 2 excluding the manually annotated docs. Models are tested on a small manually annotated subset of the data in order to verify the results of Table 2 that were measured using our automatic annotation. Numbers in **bold/blue** mark the best and second-best results, respectively.

| | | Image-to-Text | | | Text-to-Image | | | |
|-----------|-------------|---------------|--------------|--------------|---------------|--------------|--------------|--------------|
| | Name | Locked | Rec@1 | Rec@5 | Rec@10 | Rec@1 | Rec@5 | Rec@10 |
| Zero-Shot | CLIP [46] | | 14.3% | 39.3% | 55.6% | 14.7% | 36.4% | 57.0% |
| | Concatenate | | 14.2% | 40.2% | 61.6% | 11.5% | 33.6% | 51.9% |
| | Concatenate | ✓ | 9.3% | 35.4% | 58.5% | 11.7% | 31.5% | 51.5% |
| | Choose-One | | 9.8% | 39.1% | 59.9% | 13.3% | 38.2% | 59.9% |
| | Choose-One | ✓ | 12.8% | 40.5% | 59.0% | 14.2% | 41.9% | 60.0% |
| | CLIP-MIL | | 14.4% | 40.1% | 67.8% | 16.2% | 40.4% | 62.6% |
| | CLIP-MIL | ✓ | 13.9% | 41.0% | 65.0% | 15.1% | 43.2% | 60.8% |
| One-Shot | CLIP [46] | | 14.3% | 39.3% | 55.6% | 14.7% | 36.4% | 57.0% |
| | Concatenate | | 15.7% | 41.9% | 63.3% | 12.1% | 39.1% | 60.8% |
| | Concatenate | ✓ | 12.4% | 37.7% | 54.1% | 13.0% | 35.3% | 54.9% |
| | Choose-One | | 12.7% | 40.8% | 60.4% | 12.4% | 37.8% | 63.2% |
| | Choose-One | ✓ | 12.4% | 38.8% | 62.5% | 14.2% | 39.5% | 62.1% |
| | CLIP-MIL | | 16.1% | 42.7% | 66.2% | 14.6% | 43.6% | 64.0% |
| | CLIP-MIL | ✓ | 15.8% | 39.9% | 62.6% | 14.9% | 41.6% | 62.5% |
| Few-Shot | CLIP [46] | | 12.8% | 37.3% | 51.7% | 12.5% | 32.1% | 53.0% |
| | Concatenate | | 12.0% | 38.3% | 58.9% | 11.0% | 32.5% | 54.7% |
| | Concatenate | ✓ | 8.2% | 33.0% | 55.4% | 8.8% | 28.9% | 51.3% |
| | Choose-One | | 11.0% | 39.8% | 60.9% | 12.5% | 36.4% | 60.1% |
| | Choose-One | ✓ | 9.8% | 37.0% | 59.5% | 10.1% | 35.7% | 59.7% |
| | CLIP-MIL | | 13.4% | 41.3% | 61.9% | 12.7% | 38.2% | 60.5% |
| | CLIP-MIL | ✓ | 12.9% | 38.4% | 60.3% | 13.2% | 38.6% | 61.6% |
| Many-Shot | CLIP [46] | | 20.0% | 47.2% | 71.3% | 23.7% | 53.4% | 72.9% |
| | Concatenate | | 36.8% | 66.6% | 84.1% | 24.5% | 56.5% | 80.5% |
| | Concatenate | ✓ | 29.9% | 61.6% | 81.1% | 28.8% | 56.4% | 76.3% |
| | Choose-One | | 39.0% | 70.1% | 83.1% | 34.0% | 65.0% | 84.7% |
| | Choose-One | ✓ | 34.6% | 70.6% | 83.5% | 33.7% | 68.3% | 82.6% |
| | CLIP-MIL | | 43.1% | 71.4% | 83.8% | 40.7% | 67.6% | 86.5% |
| | CLIP-MIL | ✓ | 43.0% | 74.8% | 85.7% | 43.5% | 70.2% | 85.3% |

easily with adding more documents. This further highlights the benefit of automatic annotation pipeline proposed in FETA for supporting low annotation cost adaptation of V&L models to expert domains defined by corpora of documents with illustrations. **Third**, training with the MIL paradigm consistently boost performance with respect to other (non-MIL) baselines indicating the utility of using MIL and variants. **Fourth**, locked image encoder variants demonstrate interesting trade-offs with unlocked ones in different scenarios. We have further evaluated this in a more thorough ablation study of this aspect in Section 4.4, also discovering the benefit of very interesting intermediate locking options using low-rank residual adapters tuning, constituting a very exciting direction for future work. **Fifth**, overall performance levels of all baselines still leave a lot of room for improvement for future research towards practical application of FMs to (abundant) real-world expert domain application tasks. Furthermore, Table 3 validates the results in Table 2 by measuring the performance of the same baselines using a manually curated annotated documents set. The results are validated by observing the consistent performance trends between the baselines in the two tables.

4.4 Additional Ablation Study - Parameter Locking

Following [66], we evaluated the performance on our CLIP-MIL method under several parameter-locking as well as "intermediate" states. We refer to locked parameters as parameters that do not change during training. The five different options are: (i) *Unlocked*: Let both \mathcal{M}_I and \mathcal{M}_T train during fine-tuning. (ii) *Locked Image*: Lock \mathcal{M}_I and only let \mathcal{M}_T train. (iii) *Locked Text*: Lock \mathcal{M}_T

Table 4: **Parameter Locking Ablation**. This table explores different variants of locking the model parameters during MIL finetuning. We test locking the image encoder, the text encoder, or both excluding the text projection layers (Locked*) and the use of Low-Rank Adapters (LoRA) [18]. We show the interpolation between the Unlocked (rank $r = 512$) and the Locked Image (rank $r = 0$) variants by changing the rank of the added residual adapters weight matrices. This exploration clearly shows the trade-offs between locking and unlocking the image encoder MI, with up to 2.1% relative improvements in some cases. Numbers in **bold/blue** mark the best and second-best results, respectively.

| Baseline | Locking | Image-to-Text | | | Text-to-Image | | |
|----------|------------------|---------------|--------------|--------------|---------------|--------------|--------------|
| | | Rec@1 | Rec@5 | Rec@10 | Rec@1 | Rec@5 | Rec@10 |
| CLIP-MIL | Unlocked | 32.6% | 56.2% | 66.7% | 27.8% | 59.0% | 72.3% |
| | Locked Image | 34.5% | 56.8% | 66.1% | 27.2% | 57.9% | 70.2% |
| | Locked Text | 30.6% | 54.4% | 64.6% | 27.8% | 59.0% | 71.6% |
| | Locked* | 30.1% | 52.4% | 63.1% | 25.0% | 55.7% | 69.1% |
| | LoRA[18] $r=4$ | 33.8% | 57.3% | 67.6% | 28.9% | 61.4% | 74.1% |
| | LoRA[18] $r=32$ | 35.6% | 58.3% | 68.1% | 30.7% | 62.6% | 74.6% |
| | LoRA[18] $r=256$ | 35.5% | 57.7% | 67.8% | 30.8% | 62.4% | 74.4% |

and only let \mathcal{M}_I train. (iv) *Locked**: Lock both \mathcal{M}_I and \mathcal{M}_T except the last “text projection” layer in \mathcal{M}_T . (v) CLIP-LoRA as detailed in CLIP-LoRA sub section. Table 4 clearly shows the trade-offs between locking and unlocking the image encoder \mathcal{M}_I , with up to 2.1% relative improvements in some cases. More importantly this could be further significantly improved by low-rank intermediate variants with up to 2-3% additional improvement. Notice that no parameters are added as these adapters are only used for training and are fully collapsed into the model parameters at inference time. We believe that this shows that some adaptation to the full model can help.

4.5 IKEA results

Table 5 presents the results for the proposed baselines trained and tested on the IKEA dataset. For a full review of IKEA dataset see appendix section B in. For a discussion about the results, see appendix section D.5.

Table 5: **Results on IKEA dataset** using 5-fold cross-validation protocol on the entire IKEA US early manuals data. MIL based baselines obtain significant advantages over other baselines. Numbers in **bold** mark the best results while numbers in **blue** mark the second-best.

| Name | Locked | Image-to-Text | | | Text-to-Image | | | |
|----------|-------------|---------------|--------------|--------------|---------------|--------------|--------------|--------------|
| | | Rec@1 | Rec@5 | Rec@10 | Rec@1 | Rec@5 | Rec@10 | |
| All-Data | CLIP [46] | 22.9% | 43.3% | 54.2% | 25.5% | 46.8% | 59.5% | |
| | Concatenate | 6.7% | 13.7% | 18.2% | 13.2% | 27.0% | 35.9% | |
| | Concatenate | ✓ | 8.1% | 15.6% | 20.6% | 14.0% | 26.9% | 35.3% |
| | Choose-One | | 15.1% | 30.2% | 38.5% | 17.9% | 36.2% | 46.4% |
| | Choose-One | ✓ | 14.1% | 28.0% | 35.3% | 16.4% | 32.3% | 41.8% |
| | CLIP-MIL | | 26.8% | 47.7% | 57.8% | 30.1% | 54.4% | 66.2% |
| | CLIP-MIL | ✓ | 24.4% | 44.4% | 54.7% | 27.0% | 49.9% | 60.5% |

5 Related Work

Vision and Language. Many studies have recently addressed the problem of vision and language on a broad scale. Some of them focused more on text-image, such as [1, 15, 22, 31, 32, 33, 46, 53, 61, 64, 65], while others explored text-conditional image generation [41, 48, 50]. Other approaches learn strong representations from video-textual descriptions [38, 39] with or without the need for any manual annotation. The goal of these works is to learn foundational language and vision representations that are required for language and vision understanding. Unlike these works, we demonstrate here that even strong models are incapable of performing basic retrieval capabilities in technical documentation as humans do, such as diverse car service manuals and sales catalogs.

Multiple Instance Learning. Over the years, multiple instance learning methods have been applied to a variety of weakly supervised problems including: images [21, 42, 45, 54, 62, 70], videos [5, 11, 30, 37, 38, 52]. Typically, MIL methods are using different principles such as max-pooling [14], support vector machine [2], discriminative clustering [4], or even attention-based neural networks [20]. In this work, we present MIL-CLIP, an approach that combines the standard contrastive learning from CLIP [46] with multiple instance learning [14, 24, 35]. We demonstrate how this combination leads to the best performance and allows for practical applications of FMs in expert domains

Image-Text Retrieval. Image-text retrieval has been a long and well-known task with real-life applications. The two main and dominate tasks are: *image retrieval* and *text retrieval*, depending on which modality is used as the retrieved target. Previous works embedded the image and text features into a joint embedding space to calculate the similarities between them. Most of these works were trained by ranking loss [27, 59, 60], while more recent architectures and pre-training approaches [12, 46, 67] have demonstrated the potential of transformer-based models and contrastive objectives to learn image representations from text. In this work, we release a dataset containing manuals of cars and sale catalogs, showing that even large models cannot perform well on retrieval tasks, such as *image retrieval* and *text retrieval*. We hope it would pave the way for real practical applications of FMs in expert domains.

Technical and expert domains with non-natural image data. While the majority of CV literature focuses on natural images and common objects, some works have extended CV and V&L techniques to technical and expert domains (e.g., localization for autonomous driving [7], etc.). These works can be divided into works with mostly (i.) uni-modal focus, with such tasks as deep normal prediction in design sketches [16], image-to-image retrieval in patents [28, 44] (interestingly [44] also show that textual side-information can facilitate retrieval), scientific-figures classification [23], or text-to-text generation for patent claims [29]; (ii.) multi-modal works focusing on image+text reasoning tasks such as VQA on figures and InfoGraphics [10, 25, 36]. In contrast, FETA focuses on a more direct multi-modal V&L evaluation of out-of-the-box and fine-tuned, large-scale pre-trained, V&L models using text-to-image and image-to-text retrieval tasks, which are better aligned with the commonly used contrastive objectives used to pre-train V&L models. Moreover, FETA is open-ended, offering a convenient ingestion pipeline for producing automatic annotation and for the evaluation and fine-tuning of expert domains available as document corpora. This pipeline enables relatively straightforward future extensions to expert domains such as patents, figures and info-graphics.

6 Conclusion

We have proposed the first of its kind *Foundation models for Expert Task Applications* (FETA) benchmark and dataset focused on evaluating Foundation Models on expert data tasks. In our first release, FETA focuses on expert data from technical and other documents. It is accompanied with an automatic data extraction pipeline allowing for easy extension of the benchmark to larger data scales, other expert domains, and additional visual modalities by ingesting public PDF documents – an abundant data resource. FETA is accompanied with an extensive set of baselines and ablations on different training setups and finetuning strategies allowing us to conclude that: (i) Although strong on benchmarks containing common objects captured with consumer cameras, FMs still struggle with expert domain data, both due to its natural domain gap as well as absence or statistical insignificance of such data in the distribution of the massive datasets used to pre-train FMs; (ii) While our baselines still leave a lot of room for improvement contingent on future research, as expected of any good and challenging benchmark, in some situations such as many-shot fine-tuning, our best baseline performance suggests a possibility of practical application; (iii) Our diverse experimental settings help establishing best practices for fine-tuning FMs under different data regimes, and our code is easily extendable to evaluate any arbitrary FM in a similar collection of settings; (iv) Our automatic annotation pipeline and associated automatic performance metric lead to similar conclusions with regards to relative performance comparisons between different models and fine-tuning strategies, as the metric computed on the manually curated data, once again suggesting the scalability of the proposed approach to grow to larger data and additional expert tasks.

Limitations & Future Work. While the first version of FETA includes close to 150K images and texts, it is still a drop in the ocean of available technical documentation and other documents available for yet unexplored set of different expert V&L data domains. Luckily, FETA’s automatic data extraction and annotation pipeline allows to scale FETA easily. Future work includes expanding FETA to additional domains and continually evaluating new FMs as they are released to the community.

Appendix A Data Collection Details

A.1 Data Download and Conversion

Car Manuals: The car manuals data was downloaded from <https://www.workshopservicemanual.com>. Table 1 of the original paper details the amount of documents downloaded by car manufacturers. The documents contained an average of 149 pages per document.

IKEA Catalogs: The IKEA catalogs data was initially presented in [69] and downloaded from <https://github.com/ivc-yz/SSR>. The data consisted of 29 IKEA US catalogs between the years 1986 and 2005, each document contains an average of 283 pages.

The downloaded documents were processed by the DeepSearch tool <https://ds4sd.github.io/> which extracted the images and the texts. The extracted texts were further processed to create large, consecutive chunks of texts. We removed bad characters artifacts created during PDF parsing, we also filtered improbable boxes and failed boxes, finally we merged together spatially close text boxes.

The final result of our data conversion can be seen in Figures 6-8 for examples from the IKEA dataset and Figures 9-11 for examples from the Car-Manuals dataset. Red boxes mark extracted text blocks, blue boxes mark extracted images.

A.2 Identical Image Detection Process

We found that the car manual data includes images which reappear in several different locations within the same manual. Since our automatic annotation links images and texts which are located in the same page, retrieving a correct image but from a different page can artificially lower the test results. As our goal was to keep the flow unsupervised as much as possible, in order to overcome this issue we processed the images in three steps. First, we trained a self-supervised network on all the data in order to get meaningful image features. For that we used DINO [9], which we have found to create good image representations due to its loss function which inherently produces good clusters in the embedded space. As a second step, for each image we selected the top ten nearest neighbors in the embedded space. Lastly we performed Normalized Cross Correlation [63] filtering on the selected images and selected images with correlation higher than $t > 0.7$. These images were treated as identical images during test time. For the retrieval tests, the sets of texts matching to identical images were merged (by their union), and there was no penalty when retrieving an identical image from a different page. It is important to note that the DINO model used for identical images filtering was used only for that and not used in our experiments in any other way.

A.3 Text bounding box merging

OCR engines sometimes fail in parsing full paragraphs and end up splitting them to numerous bounding boxes. In order to lessen the effect such OCR errors has on FETA, we use a mechanism to merge adjacent bounding boxes into one bounding box. The process has 2 stages, in the first stage we employ a dilation technique in which we increase the length of each of the box's horizontal edges by a constant which is a percentage of the page's horizontal length (we used 1%), we also increase the length of each box's vertical edge by a bigger constant (4* times the horizontal constant) as text bounding boxes tend to be wide and short. This creates some overlaps between neighboring boxes. In the second stage we merge all the boxes which has any kind of overlap between them. Each group of overlapping boxes are merged into a bounding box that minimally contains the boxes being merged.

A.4 Manual Annotation Statistics

We created manual annotations for part of the Car Manuals dataset. Our manually labeled data consists of 15 documents and has 449 image-text pairs. We randomly selected these 15 documents, making sure to select at least two documents from each manufacturer. We then manually selected up to 50 images per document and manually generated (by a human expert) the image description using the information on the page as technical reference. This annotation was used to both validate the test results obtained on the automatically curated data and demonstrate that pre-training on automatically curated data indeed improves results on manually annotated data (Table 3 in the main paper). From

Tables 2 and 3 in the main paper show that the same trends in terms of relative performance of different baselines appear both on the manual and the automatically curated data.

A.5 Further details on the automatic annotation

Figure 2 show the main steps in creating our automatic annotation of images - texts bags, the figure demonstrate the automatic process from a zip of PDFs to bags annotations which enable MIL training and test on the data. The steps are shown on an example pages from the cars dataset. The images above the flow chart show the creation of image-texts bags, while the images below the flow chart shot the creation of text-images bags.

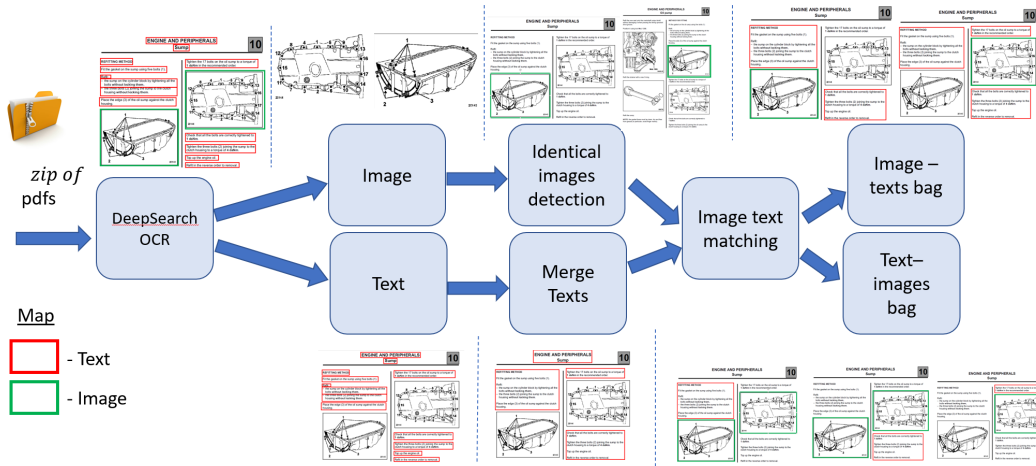


Figure 2: **Simplified figure explaining the automatic annotation process** showed using an example page from the cars dataset.

Appendix B Additional data analysis

B.1 Automatic vs manual text annotations cover

In order to assess the quality of the automatic annotations, we compare here between the manual annotations and automatic annotations. In this test we consider only the manually annotated documents. We report the percentage of the times, when looking at a specific image, the manually annotated text is contained within the automatically extracted texts for that same image (with a significant overlap). Over the cars data the cover is 93 percent. This high overlap is aligned with the Multiple Instance Learning setting where the MIL bag is assumed to contain at least one true sample. We consider the remainder or 7% as annotation noise. In the future versions of FETA it would be possible to increase this coverage by considering extracting text from adjacent pages, as well as using PDF sections parsing results.

B.2 Data quality check

We have asked three external reviewers to go over a subset of the automatic annotations. Each reviewer was asked to rate the annotation as good or bad, we present the findings of this experiment in Table 6.

Table 6: **Data quality check of automatic annotations**

| | Good (out of 3) | | |
|-----------------------|-----------------|-------|-------|
| | 1+ | 2+ | 3 |
| Automatic annotations | 93.6% | 90.2% | 82.3% |

B.3 Data statistics and comparison to other datasets

In order to further demonstrate the difference and resemblance between cars and IKEA data sets to each and to other popular data sets, we show some data statistics in Table 7, all tokens data was calculated by us using CLIP’s tokenizer. Word count to vocabulary size was calculated as the number of words occurrences in the entire dataset divided by a set of all unique words, present in the dataset, all number except CC3M(taken from original paper) were calculated by us. Image-page ratio reports the ratio between image area to entire page area in the dataset.

Table 7: **Data Statistics** In this table we compare the statistics of the texts in the Car-Manuals and IKEA datasets to common V&L datasets, i.e COCO, Flickr30K and CC3M

| Measure | Cars | IKEA | Flickr30k | COCO | CC3M |
|-------------------------------|-------|-------|-----------|-------|---------|
| Mean tokens per caption | 44.2 | 59.1 | 15.7 | 13.5 | 10.3 |
| Std tokens per caption | 67.3 | 83.9 | 5.6 | 2.7 | 4.5 |
| Unique tokens | 11152 | 14942 | 15351 | 17624 | 51201 |
| Average words per image | 79.5 | 208.9 | 66.9 | 53 | 51.5 |
| Word count to vocabulary size | 48.3 | 14.3 | 87.4 | 97.2 | 804.8 |
| Total images number | 52119 | 9574 | 31783 | 82783 | 3318333 |

B.4 Common nouns and adjectives in data

To further understand the difference between the Car-Manuals and IKEA datasets to each other and to other popular datasets we report the most common nouns and adjectives present in each dataset sorted by appearance count. As can be seen in Figures 3 and 4 and in Tables 8 and 9, the nouns and adjectives from Flickr30K, COCO, CC3M are very similar and all three include nouns such as: person, beach etc. also, they all use the same adjectives such as white, young, etc. It seems that those 3 very popular datasets all reside in a very close domain and treat the same kind of popular data of natural images. When looking at the nouns and adjectives in Cars and IKEA, we see nouns such as: engine, connector, table, cotton which are specific to the expert domain each dataset deals with. We also see adjectives like, diagnostic, new, solid, adjustable which are again a strong characteristic of the expert domains of Cars and IKEA. The resemblance between Flickr30K, COCO and CC3M, coupled with the difference between them to our Cars and IKEA datasets, further strengthen our claim that FETA can indeed be useful in order to expand current FMs research to new under studied domains of expert V&L tasks which may provide noticeable value for practical real world applications.

Table 8: **Most common nouns by dataset** ordered by count from left to right.

| Dataset | Most Common Nouns |
|-----------|--|
| Cars | engine, switch, connector, control, front, harness, oil, air, fuel, installation, system, rear, caution, ignition, position, vehicle, side, ground, terminal, brake, door, unit, cylinder. |
| IKEA | table, steel, bed, cotton, glass, frame, cover, storage, designer, pine, finish, unit, design, sofa, chair, shelf, cabinet, plastic, birch, veneer, wall, door, seat, lamp, set |
| Flickr30K | man, woman, people, shirt, girl, boy, men, dog, street, child, women, person, water, children, group of people, hat, background, beach, ball, sidewalk. |
| COCO | man, people, woman, person, group, table, street, tennis, train, dog |
| CC3M | person, actor, artist, player, premiere, football, woman, beach, game, girl |

B.5 Choice of evaluation metric

We chose the text-to-image and image-to-text retrieval task for two main reasons: This metric is directly aligned with the popular contrastive training objective used for most of V&L models (e.g. CLIP or FLAVA) and as such should be their strongest suit. We however show that even under this metric CLIP under performs on FETA expert tasks compared to its performance demonstrated for e.g. photos of common objects. This metric is also possible to compute when regarding the automatic annotation process. In our automatic process, little is known a priori about the data. The assumption that co-location of text and images is strongly correlated with the semantics is a relatively general

Table 9: **Most common adjectives by dataset** ordered by count from left to right.

| Dataset | Most Common Adjectives |
|-----------|--|
| Cars | new, open, diagnostic, necessary, short, upper, main, idle, high, other, normal, low, electric, manual, same, negative, positive, active, foreign, hot, old |
| IKEA | white, solid, black, clear, easy, adjustable, new, red, available, high, limited, green, washable, removable, extra, natural, low, last, soft, other, different, full, good, |
| Flickr30K | young, white, black, blue, red, little, green, other, large, yellow, small, brown, older, several, asian, gray, old, many, blond, dark. |
| COCO | white, two, large, small, front, red, young, black, young, |
| CC3M | white, young, day, black, red, blue, old, new, night, green, first, front |



Figure 3: A Visual representation of the most common nouns in the Car-Manuals and IKEA datasets, compared to COCO, Flickr30K, and CC3M

assumption. As shown in our Results in section 4.3 and in Table 3 of the main paper, our choice of automatic metric is valid as it gives the same conclusions using the same models and baselines performance as evaluated on the manually annotated and curated data.



Figure 4: A Visual representation of the most common adjectives in the Car-Manuals and IKEA datasets, compared to COCO, Flickr30K, and CC3M

Appendix C Additional Implementation Details

Training Epochs: In general we train all MIL variants for 20 epochs, however we found that for the Zero-Shot and Few-Shot settings of the car manuals data we found that this amount results in over-fitting. We thus trained these two settings with only two epochs which we found to yield the best results.

Appendix D Additional results

D.1 MIL Variants Ablation

In Section 3.2 of the paper we discussed several options for training CLIP under the MIL setting. Table 10 shows the performance for the three MIL variants on the Few-Shot and Many-Shot test settings. These results confirm that in the majority of the cases, MIL-NCE achieves the highest performing results. We therefore chose to use this MIL variant in all of experiments in the main paper where the MIL baselines are evaluated.

Table 10: **MIL Variant Ablations:** Image-to-Text and Text-to-Image retrieval accuracy for three MIL fine-tuning baseline variants under two different data-split settings. Our experimental settings is the same as Table 2 from the main paper but only include Many-Shot and Few-Shot (the more practical settings). The "Locked" column refers to versions trained with locked (frozen) parameters of the image encoder \mathcal{M}_I . Numbers in **bold** mark the best results while numbers in **blue** mark the second-best.

| | | Image-to-Text | | | Text-to-Image | | | |
|-----------|------------------|---------------|--------------|--------------|---------------|--------------|--------------|--------------|
| | Name | Locked | Rec@1 | Rec@5 | Rec@10 | Rec@1 | Rec@5 | Rec@10 |
| Few-Shot | CLIP-MIL-SOFTMAX | | 14.6% | 34.4% | 47.5% | 13.4% | 34.7% | 47.8% |
| | CLIP-MIL-SOFTMAX | ✓ | 13.4% | 33.5% | 46.6% | 12.2% | 34.1% | 47.8% |
| | CLIP-MIL-MAX | | 13.7% | 34.5% | 47.8% | 15.7% | 34.8% | 48.4% |
| | CLIP-MIL-MAX | ✓ | 13.5% | 33.9% | 46.4% | 12.3% | 34.7% | 48.5% |
| | CLIP-MIL-NCE | | 14.1% | 36.7% | 48.9% | 15.0% | 35.2% | 50.0% |
| | CLIP-MIL-NCE | ✓ | 13.8% | 33.7% | 47.5% | 11.6% | 33.0% | 47.0% |
| Many-Shot | CLIP-MIL-SOFTMAX | | 32.0% | 54.8% | 65.7% | 26.5% | 58.1% | 71.3% |
| | CLIP-MIL-SOFTMAX | ✓ | 34.1% | 56.5% | 66.4% | 26.7% | 58.0% | 70.3% |
| | CLIP-MIL-MAX | | 34.4% | 56.7% | 66.2% | 27.3% | 57.9% | 71.1% |
| | CLIP-MIL-MAX | ✓ | 31.2% | 54.7% | 65.7% | 26.2% | 58.1% | 71.3% |
| | CLIP-MIL-NCE | | 32.6% | 56.2% | 66.7% | 27.8% | 59.0% | 72.3% |
| | CLIP-MIL-NCE | ✓ | 34.5% | 56.8% | 66.1% | 27.2% | 57.9% | 70.7% |

D.2 CLIP Architecture

In this section we present equivalent results to Table 2 from the main paper, using the ViT-L/14 backbone instead of ResNet50. Table 11 shows consistent baseline relative comparison results with the results presented in Table 2 of the main paper. As we can see from Table 11, using the ViT-L/14 backbone leads to higher performance (compared to ResNet50) with the CLIP-MIL options maintaining their significant gains under this stronger backbone.

D.3 Evaluating Additional Foundation Model

In Table 2 of the main paper we have added the evaluation of three of the strongest performing and the most recent of the openly available foundation models - FLAVA [53], ALBEF[32] and ViT[26] to our set of Car-Manuals data evaluations comparing it to CLIP and our MIL baselines. For FLAVA, We used the released pre-trained FLAVA model available on Huggingface: https://huggingface.co/docs/transformers/model_doc/flava. We used facebook/flava-full pre-trained model. We evaluated both *contrastive* and *ITM* matching scores available in FLAVA and report results for the contrastive score, as it produced better results in all evaluations. We observe that stronger

Table 11: **Results using ViT-L/14 backbone** pre-trained by CLIP. Using the ViT-L/14 backbone leads to higher performance (compared to ResNet50) with the CLIP-MIL options maintaining their significant gains under this stronger backbone. Numbers in **bold** mark the best results while numbers in **blue** mark the second-best.

| | Image-to-Text | | | | Text-to-Image | | | |
|-----------|---------------|--------|--------------|--------------|---------------|--------------|--------------|--------------|
| | Name | Locked | Rec@1 | Rec@5 | Rec@10 | Rec@1 | Rec@5 | Rec@10 |
| Zero-Shot | CLIP [46] | | 11.8% | 29.5% | 41.1% | 12.0% | 32.6% | 46.6% |
| | Concatenate | | 12.0% | 31.8% | 44.6% | 11.7% | 31.7% | 45.1% |
| | Concatenate | ✓ | 12.2% | 32.0% | 44.6% | 10.6% | 30.8% | 44.5% |
| | Choose-One | | 12.7% | 31.4% | 43.0% | 11.8% | 31.9% | 46.0% |
| | Choose-One | ✓ | 12.8% | 31.6% | 44.6% | 11.2% | 31.6% | 45.3% |
| | CLIP-MIL | | 13.6% | 32.9% | 46.5% | 13.2% | 34.2% | 47.8% |
| | CLIP-MIL | ✓ | 14.0% | 33.5% | 46.3% | 13.1% | 34.3% | 47.4% |
| One-Shot | CLIP [46] | | 11.8% | 29.5% | 41.1% | 12.0% | 32.6% | 46.6% |
| | Concatenate | | 12.8% | 24.4% | 35.8% | 11.4% | 31.7% | 45.9% |
| | Concatenate | ✓ | 13.3% | 33.8% | 46.2% | 11.2% | 31.4% | 45.2% |
| | Choose-One | | 12.6% | 32.2% | 44.4% | 11.8% | 32.3% | 46.5% |
| | Choose-One | ✓ | 13.2% | 32.9% | 44.6% | 11.7% | 32.4% | 46.6% |
| | CLIP-MIL | | 14.2% | 34.4% | 46.8% | 13.7% | 35.1% | 49.2% |
| | CLIP-MIL | ✓ | 14.5% | 35.3% | 47.2% | 13.0% | 34.4% | 48.1% |
| Few-Shot | CLIP [46] | | 10.7% | 28.7% | 40.6% | 11.2% | 30.8% | 44.9% |
| | Concatenate | | 10.5% | 31.2% | 44.7% | 11.9% | 30.9% | 46.9% |
| | Concatenate | ✓ | 12.0% | 31.5% | 44.9% | 13.0% | 34.1% | 48.7% |
| | Choose-One | | 14.7% | 37.7% | 51.7% | 13.8% | 36.3% | 51.3% |
| | Choose-One | ✓ | 12.9% | 32.1% | 45.1% | 11.9% | 33.5% | 47.5% |
| | CLIP-MIL | | 19.1% | 44.2% | 56.8% | 15.8% | 41.0% | 56.1% |
| | CLIP-MIL | ✓ | 19.1% | 40.7% | 53.3% | 17.3% | 40.3% | 53.8% |
| Many-Shot | CLIP [46] | | 15.7% | 32.8% | 43.2% | 15.5% | 39.7% | 53.5% |
| | Concatenate | | 15.1% | 32.1% | 44.7% | 14.3% | 39.4% | 54.8% |
| | Concatenate | ✓ | 20.8% | 37.6% | 49.3% | 19.0% | 45.6% | 60.3% |
| | Choose-One | | 24.1% | 49.1% | 61.1% | 21.9% | 53.3% | 68.4% |
| | Choose-One | ✓ | 30.9% | 57.0% | 67.9% | 24.4% | 57.3% | 71.5% |
| | CLIP-MIL | | 31.2% | 55.2% | 66.2% | 27.3% | 60.1% | 73.3% |
| | CLIP-MIL | ✓ | 40.1% | 61.9% | 71.0% | 33.6% | 65.1% | 76.8% |

(relative to CLIP) common-objects performance reported by FLAVA, does not translate to improved numbers on FETA expert car manuals task. For ALBEF and ViT we have used the the VL-Checklist git repository [68]. We have used their code in order to obtain image-text scores between all image texts pairs in each document and used them in our retrieval test. As with FLAVA, the results for ALBEF and ViT are lower than CLIP and these models struggle in zero-shot performance on our data. We believe that this further supports our hypothesis that FMs need to be fine-tuned on the expert tasks as their out-of-the-box performance on these tasks is low. This is most likely due to bias towards common as is stated in the main paper. These experiments underline the need for our proposed FETA benchmark in order to improve the applicability of FMs to practical real-world problems often involving specialized expert V&L data.

D.4 Pre-trained CLIP vs Training from Scratch

All of the experiments presented in the main paper and the supplementary material initialize the training from a pre-trained CLIP model trained on 400M image-text pairs. In this section we examine the effect of training the ResNet50 CLIP model from scratch on the car manuals dataset. Table 12 shows the result and compares the same model trained from scratch vs starting from a pre-trained CLIP model. We also include the locked and unlocked versions of the visual encoder. The advantage of starting from a strong pre-trained model is clear and raises the assumption that starting from a

better pre-trained model will yield better results, also verified by the experiments using ViT-L/14 CLIP architecture in section D.2.

Table 12: **Initializing with a Pre-trained CLIP400M VS from Scratch**. Numbers in **bold** mark the best results while numbers in **blue** mark the second-best.

| | | Image-to-Text | | | | | Text-to-Image | | |
|-----------|----------|---------------|--------|--------------|--------------|--------------|---------------|--------------|--------------|
| | Name | Pre-traind | Locked | Rec@1 | Rec@5 | Rec@10 | Rec@1 | Rec@5 | Rec@10 |
| Zero-Shot | CLIP-MIL | ✓ | | 10.5% | 34.0% | 48.5% | 11.7% | 32.9% | 47.9% |
| | | ✓ | ✓ | 11.0% | 29.2% | 40.0% | 9.7% | 28.1% | 40.6% |
| | | | ✓ | 3.4% | 13.5% | 23.0% | 3.2% | 16.3% | 30.1% |
| | | | | 4.2% | 14.3% | 24.6% | 3.9% | 18.3% | 31.0% |
| One-Shot | CLIP-MIL | ✓ | | 11.0% | 30.3% | 43.2% | 9.9% | 27.9% | 40.9% |
| | | ✓ | ✓ | 11.9% | 30.3% | 42.5% | 10.9% | 29.4% | 43.2% |
| | | | ✓ | 5.2% | 16.9% | 28.1% | 4.4% | 19.2% | 32.9% |
| | | | | 5.3% | 16.9% | 27.4% | 4.3% | 17.8% | 31.0% |
| Few-Shot | CLIP-MIL | ✓ | | 14.1% | 36.7% | 48.9% | 15.0% | 35.2% | 50.0% |
| | | ✓ | ✓ | 13.8% | 33.7% | 47.5% | 11.6% | 33.0% | 47.0% |
| | | | ✓ | 8.4% | 25.1% | 37.8% | 6.7% | 25.0% | 39.0% |
| | | | | 8.5% | 24.9% | 36.0% | 6.1% | 23.4% | 36.6% |
| Many-Shot | CLIP-MIL | ✓ | | 32.6% | 56.2% | 66.7% | 27.8% | 59.0% | 72.3% |
| | | ✓ | ✓ | 34.5% | 56.8% | 66.1% | 27.2% | 57.9% | 70.7% |
| | | | ✓ | 29.1% | 48.6% | 58.1% | 25.0% | 52.3% | 65.2% |
| | | | | 24.7% | 44.5% | 54.7% | 19.3% | 46.6% | 61.4% |

D.5 IKEA US yearly catalogues

The IKEA data represents a different expert task - one of large-scale sales inventory (thousands of items). As with the technical documentation, sales catalogues naturally populate the long-tail of the common-objects biased data distributions used to train foundation models. Table 5 presents the results for the proposed baselines trained and tested on the IKEA dataset. Since in this case there are no distinct manufacturers and we did not like to partition on different yearly fashion styles due to their inconsistent nature, we followed a simple 5-fold cross-validation protocol using the entire IKEA data. Notably the IKEA dataset was processed using the same pipeline as the car manuals verifying the scalability of the proposed automatic annotation approach. As for the car manuals, also on IKEA data MIL based baselines obtaining significant advantages over other baselines. Interestingly, on IKEA data we also observe that both strategies that avoid direct use of the multiple annotation hypotheses (Concatenate and Choose-One) not only under-perform the MIL baselines, but also worsen the results relative to the CLIP baseline. This is likely due to sharper distinction between different associated text hypotheses, with only one of them being correct and other not only unrelated, but even belonging to other objects on the same (commonly densely packed) page. In such situation, non-MIL solutions are in significant disadvantage since as opposed to MIL they do not consider all the options at once with the logically accurate OR relation between possible labels, thus leading the model astray with wrongful gradient updates using losses computed with incorrect labels.

D.6 Single fold reference results for quicker evaluation by future benchmark users

All experiments in the paper and other parts of this supplementary were performed using 5-fold cross-validation. Yet it is time consuming to evaluate many models 5 times. Therefore, as a service to the future users of our proposed FETA benchmark, we also provide reference results for a single fold out of the 5 we defined for the full evaluation. Single fold results for our Car-Manuals dataset is presented in Table 13 and for our IKEA dataset is presented in Table 14. As can be seen from the tables, the relative performance trends are preserved also in this single fold evaluation and hence it can serve as a reference for quicker evaluation for future users, before they run the full evaluation that takes 5 times longer. We provide a script to run this exact fold split in our code package for reproducibility.

Table 13: **Car-Manuals dataset single fold reference results for quicker evaluation by future benchmark users.** Provided as a service to the future users of our proposed FETA benchmark by stating a 5 times faster (then full 5-fold cross val.) benchmark to compute reproducible evaluation reference point. Intended to facilitate faster evaluation & debugging of new methods. The exact split is enclosed in the benchmark code. Numbers in **bold** mark the best results while numbers in **blue** mark the second-best.

| | Name | Locked | Image-to-Text | | | Text-to-Image | | |
|-----------|-------------|--------|---------------|--------------|--------------|---------------|--------------|--------------|
| | | | Rec@1 | Rec@5 | Rec@10 | Rec@1 | Rec@5 | Rec@10 |
| Zero-Shot | CLIP [46] | | 9.7% | 26.8% | 38.1% | 10.2% | 26.7% | 39.5% |
| | Concatenate | | 6.5% | 20.4% | 31.5% | 7.1% | 25.0% | 38.4% |
| | Concatenate | ✓ | 9.4% | 25.0% | 36.7% | 8.1% | 24.0% | 37.6% |
| | Choose-One | | 7.2% | 21.1% | 32.9% | 6.3% | 22.0% | 35.6% |
| | Choose-One | ✓ | 7.1% | 21.7% | 33.9% | 6.6% | 22.0% | 34.1% |
| | CLIP-MIL | | 11.7% | 29.8% | 42.4% | 10.8% | 30.4% | 44.3% |
| | CLIP-MIL | ✓ | 11.0% | 28.5% | 40.6% | 9.7% | 28.2% | 40.8% |
| One-Shot | CLIP [46] | | 9.7% | 26.8% | 38.1% | 10.2% | 26.7% | 39.5% |
| | Concatenate | | 7.3% | 22.0% | 33.5% | 7.6% | 24.7% | 39.6% |
| | Concatenate | ✓ | 7.1% | 20.5% | 32.8% | 6.9% | 23.6% | 37.9% |
| | Choose-One | | 6.8% | 23.3% | 34.8% | 6.1% | 21.7% | 34.7% |
| | Choose-One | ✓ | 8.3% | 23.9% | 36.2% | 6.4% | 21.6% | 34.9% |
| | CLIP-MIL | | 10.1% | 28.5% | 40.5% | 10.8% | 28.2% | 41.8% |
| | CLIP-MIL | ✓ | 9.7% | 27.9% | 40.8% | 9.0% | 26.2% | 38.4% |
| Few-Shot | CLIP [46] | | 8.7% | 25.6% | 37.3% | 9.3% | 24.4% | 36.7% |
| | Concatenate | | 6.9% | 24.8% | 38.2% | 10.7% | 29.6% | 45.4% |
| | Concatenate | ✓ | 9.6% | 23.0% | 35.0% | 10.3% | 30.1% | 42.1% |
| | Choose-One | | 14.4% | 32.3% | 46.3% | 10.7% | 29.6% | 46.7% |
| | Choose-One | ✓ | 12.4% | 35.9% | 49.5% | 11.6% | 29.0% | 44.2% |
| | CLIP-MIL | | 16.1% | 40.7% | 54.0% | 14.1% | 36.6% | 53.1% |
| | CLIP-MIL | ✓ | 14.6% | 36.6% | 48.8% | 12.6% | 31.5% | 48.5% |
| Many-Shot | CLIP [46] | | 13.8% | 31.2% | 41.6% | 13.7% | 36.4% | 50.7% |
| | Concatenate | | 18.9% | 38.1% | 48.0% | 16.9% | 44.7% | 59.9% |
| | Concatenate | ✓ | 19.2% | 38.0% | 49.2% | 15.8% | 40.3% | 54.9% |
| | Choose-One | | 21.6% | 47.1% | 60.4% | 19.9% | 52.3% | 66.7% |
| | Choose-One | ✓ | 26.9% | 52.6% | 63.7% | 21.0% | 52.3% | 66.5% |
| | CLIP-MIL | | 33.2% | 56.0% | 66.7% | 28.0% | 61.1% | 73.2% |
| | CLIP-MIL | ✓ | 34.5% | 58.4% | 66.5% | 28.0% | 59.7% | 71.8% |

D.7 Median Results of Main Table 2

For completion we add the results of Few-Shot and Many-Shot settings from table 2 of the main manuscript with the difference of using Median instead of average. Results are presented in 15. As can be seen the results follow the same trend as table 2 from the main manuscript.

D.8 Illustrative explanation of our MIL variants

In Figure 5 we give an illustrative explanation of our MIL methods. Our MIL variant is composed of many to many MIL, many images to many texts, for the sake of simplicity we show here one to many MIL, image to texts MIL. Text to images MIL is very similar and thus not displayed. Each MIL block in the figure receives as inputs one image and many texts, a bag of positive texts chosen by our automatic annotation process and many negative texts taken from other pages the dataset. The output is detailed in Figure 5 and is used for the calculation of the loss. The figure is a schematic flowchart created for the purpose of intuition, the exact specifications of those losses are explained in Section 3 of the main paper.

Table 14: **IKEA dataset single fold results** Numbers in **bold** mark the best results while numbers in **blue** mark the second-best.

| | | Image-to-Text | | | Text-to-Image | | | |
|----------|-------------|---------------|--------------|--------------|---------------|--------------|--------------|--------------|
| | Name | Locked | Rec@1 | Rec@5 | Rec@10 | Rec@1 | Rec@5 | Rec@10 |
| All-Data | CLIP [46] | | 22.9% | 43.3% | 54.3% | 25.5% | 46.9% | 59.5% |
| | Concatenate | | 8.4% | 15.1% | 18.7% | 13.6% | 27.2% | 36.7% |
| | Concatenate | ✓ | 9.8% | 17.4% | 21.9% | 14.9% | 27.1% | 35.6% |
| | Choose-One | | 15.5% | 32.4% | 41.7% | 18.1% | 35.5% | 45.0% |
| | Choose-One | ✓ | 15.3% | 29.6% | 38.0% | 16.6% | 32.3% | 41.8% |
| | CLIP-MIL | | 28.0% | 49.4% | 59.0% | 28.6% | 53.5% | 65.4% |
| | CLIP-MIL | ✓ | 26.3% | 45.8% | 55.9% | 26.8% | 49.7% | 61.3% |

Table 15: **Median results of Table 2 of the manuscript** Image-to-Text and Text-to-Image retrieval accuracy, same models and settings as in Table 2 but using median instead of average. Numbers in **bold** mark the best results while numbers in **blue** mark the second-best.

| | | Image-to-Text | | | Text-to-Image | | | |
|-----------|-------------|---------------|--------------|--------------|---------------|--------------|--------------|--------------|
| | Name | Locked | Rec@1 | Rec@5 | Rec@10 | Rec@1 | Rec@5 | Rec@10 |
| Few-Shot | CLIP [46] | | 9.1% | 25.5% | 36.2% | 9.9% | 23.7% | 35.6% |
| | Concatenate | | 8.5% | 24.2% | 39.8% | 10.2% | 29.8% | 45.1% |
| | Concatenate | ✓ | 8.4% | 23.3% | 37.2% | 10.0% | 27.8% | 40.6% |
| | Choose-One | | 11.1% | 29.9% | 44.3% | 12.1% | 33.4% | 46.2% |
| | Choose-One | ✓ | 11.7% | 31.2% | 44.2% | 10.0% | 29.6% | 43.7% |
| | CLIP-MIL | | 11.9% | 33.9% | 50.9% | 14.3% | 35.3% | 53.1% |
| | CLIP-MIL | ✓ | 10.6% | 31.3% | 46.9% | 9.9% | 30.9% | 47.4% |
| Many-Shot | CLIP [46] | | 13.8% | 31.2% | 41.6% | 16.6% | 36.4% | 50.7% |
| | Concatenate | | 18.4% | 38.1% | 49.3% | 16.1% | 43.4% | 59.6% |
| | Concatenate | ✓ | 20.2% | 40.1% | 51.2% | 16.5% | 41.8% | 59.9% |
| | Choose-One | | 24.6% | 50.9% | 62.9% | 21.1% | 53.0% | 67.6% |
| | Choose-One | ✓ | 28.0% | 53.3% | 64.8% | 22.2% | 52.9% | 67.1% |
| | CLIP-MIL | | 31.8% | 56.0% | 66.7% | 27.9% | 59.4% | 72.3% |
| | CLIP-MIL | ✓ | 34.3% | 56.3% | 66.1% | 27.3% | 58.4% | 71.2% |

Appendix E License

This dataset is freely available: it can be redistribute under the terms of the GNU General Public License (version 3) as published by the Free Software Foundation.

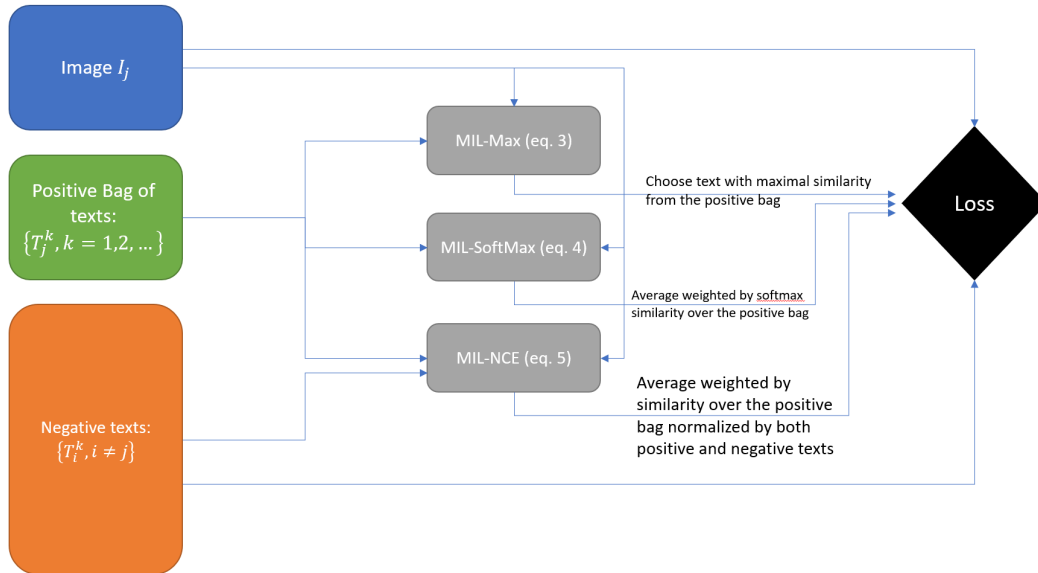


Figure 5: **Illustrative explanation of our MIL variants:** An example of one way MIL, from one image to a bag of texts. The figure is added for intuition only, the accurate details are in main paper section 3.



Figure 6: **Examples from the IKEA dataset:** In this example we can see the bounding box of all the detected texts withing the page marked in a red box. The images are marked in a blue box.

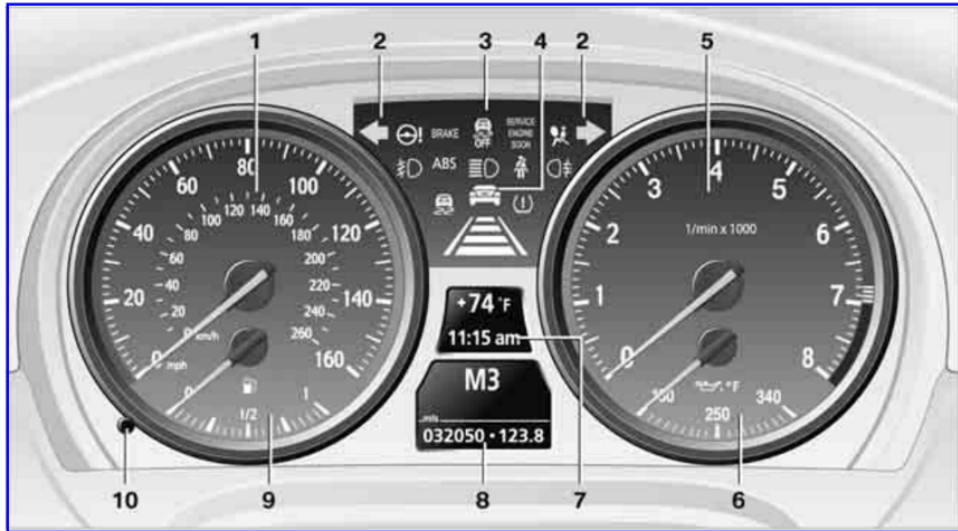


Figure 7: Examples from the IKEA dataset: In this example we can see the bounding box of all the detected texts within the page marked in a red box. The images are marked in a blue box.



Figure 8: Examples from the IKEA dataset: In this example we can see the bounding box of all the detected texts within the page marked in a red box. Only the images are marked in a blue box.

Instrument cluster



- 1 Speedometer
- 2 Indicator lamps for turn signals
- 3 Indicator and warning lamps [13](#)
- 4 Displays for Active Cruise Control [75](#)
- 5 Tachometer [83](#)
- 6 Engine oil temperature [83](#)
- 7 Display for
 - ▷ Clock [82](#)
 - ▷ Outside temperature [82](#)
 - ▷ Indicator and warning lamps [92](#)

- 8 Display for
 - ▷ Position of automatic transmission [64](#)
 - ▷ Gear indicator of 7-gear Sport automatic transmission with double clutch [66](#)
 - ▷ Computer [84](#)
 - ▷ Date of next scheduled service, and remaining distance to be driven [87](#)
 - ▷ Odometer and trip odometer [82](#)
 - ▷ High-beam Assistant [113](#)
 - ▷ Checking the oil level [260](#)
 - ▷ Settings and information [86](#)
 - ▷ ▲ There is a Check Control message [92](#)
- 9 Fuel gauge [83](#)
- 10 Resetting the trip odometer [82](#)

Figure 9: **Examples from the expert car manuals dataset:** In this example we can see the bounding box of all the detected texts withing the page marked in a red box. The images are marked in a blue box.

iDrive

Vehicle equipment

In this chapter, all production, country, and optional equipment that is offered in the model range is described. For this reason, descriptions will be given of some equipment that may not be available in a vehicle, for example due to the special options or national-market version selected. This also applies to safety related functions and systems.

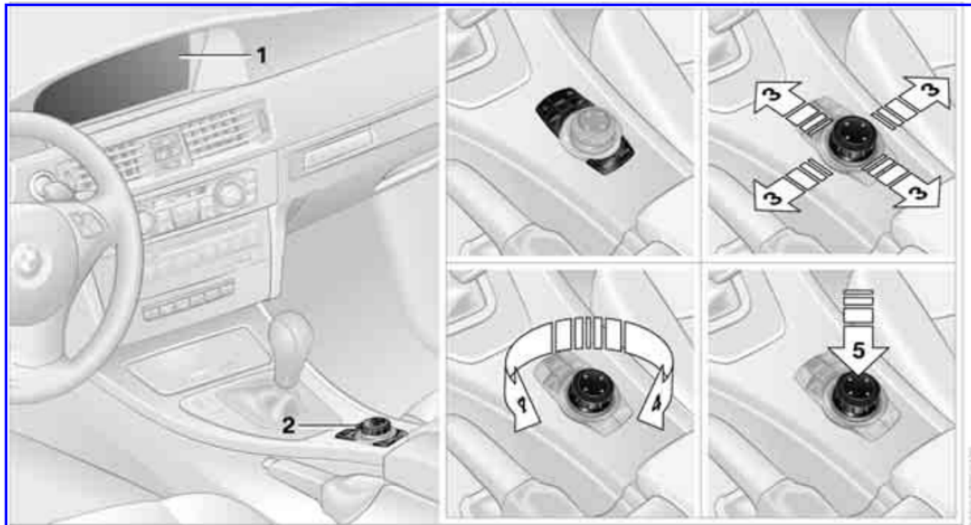
The concept

iDrive integrates the functions of a large number of switches. This allows these functions to be operated from a single central position.

⚠ Make entries only when traffic and road conditions permit; otherwise, you may endanger vehicle occupants and other road users by being distracted. ◀


Controls at a glance


Controls



- | | |
|--|---|
| <p>1 Control Display</p> <p>2 Controller with buttons You can use the buttons to open the menus directly. The controller can be used to select the menu items and create settings.</p> | <p>▷ Move in four directions, arrows 3</p> <p>▷ Turn, arrow 4</p> <p>▷ Push, arrow 5</p> |
|--|---|

Figure 10: **Examples from the expert car manuals dataset:** In this example we can see the bounding box of all the detected and **associated** texts withing the page marked in a **red** box. The images are marked in a **blue** box.

 The warning lamp in the instrument cluster lights up while the engine is running: the remote control is no longer inside the vehicle. After the engine is switched off, the engine can only be restarted within approx. 10 seconds.

 The indicator lamp in the instrument cluster lights up and a message appears on the Control Display: replace the battery in the remote control.


Replacing the battery

The remote control for Comfort Access contains a battery that will need to be replaced from time to time.


1. Take the integrated key out of the remote control, refer to page 30.



2. Remove the cover.
3. Insert the new battery with the plus side facing up.
4. Press the cover on to close.

 Dispose of the old battery at a collection point or at your BMW center. ◀

Windows

 To prevent injuries, watch the windows while closing them. Take the remote control with you when you leave the car; otherwise, children could operate the electric windows and possibly injure themselves. ◀

Coupe: opening, closing



- ▶ Press the switch to the resistance point: The window opens as long as you press the switch.
- ▶ Press the switch beyond the resistance point: The window opens automatically. Press the switch again to stop the opening movement.

You can close the windows in the same manner by pulling the switch.

Convertible: opening, closing

Individually



- ▶ Press the switch to the resistance point: The window opens as long as you press the switch.
- ▶ Press the switch beyond the resistance point: The window opens automatically. Press the switch again to stop the opening movement.

You can close the windows in the same manner by pulling the switch. The rear windows do not close automatically.

Figure 11: **Examples from the expert car manuals dataset:** In this example we can see the bounding box of all the detected and **associated** texts withing the page marked in a **red** box. One image is marked in a **blue** box.

References

- [1] Jean-Baptiste Alayrac, Jeff Donahue, Pauline Luc, Antoine Miech, Iain Barr, Yana Hasson, Karel Lenc, Arthur Mensch, Katie Millican, Malcolm Reynolds, Roman Ring, Eliza Rutherford, Serkan Cabi, Tengda Han, Zhitao Gong, Sina Samangooei, Marianne Monteiro, Jacob Menick, Sebastian Borgeaud, Andrew Brock, Aida Nematzadeh, Sahand Sharifzadeh, Mikolaj Binkowski, Ricardo Barreira, Oriol Vinyals, Andrew Zisserman, and Karen Simonyan. Flamingo: a visual language model for few-shot learning, 2022. 1, 9
- [2] Stuart Andrews, Ioannis Tsochantaridis, and Thomas Hofmann. Support vector machines for multiple-instance learning. In *NIPS*, 2002. 10
- [3] Christoph Auer, Michele Dolfi, André Carvalho, Cesar Berrospi Ramis, and Peter W. J. Staar. Delivering document conversion as a cloud service with high throughput and responsiveness, 2022. 3
- [4] Francis Bach and Zaïd Harchaoui. Difffrac: a discriminative and flexible framework for clustering. In J. Platt, D. Koller, Y. Singer, and S. Roweis, editors, *Advances in Neural Information Processing Systems*, volume 20. Curran Associates, Inc., 2007. 10
- [5] Piotr Bojanowski, Francis R. Bach, Ivan Laptev, Jean Ponce, Cordelia Schmid, and Josef Sivic. Finding actors and actions in movies. *2013 IEEE International Conference on Computer Vision*, pages 2280–2287, 2013. 10
- [6] Rishi Bommasani, Drew A. Hudson, Ehsan Adeli, Russ Altman, Simran Arora, Sydney von Arx, Michael S. Bernstein, Jeannette Bohg, Antoine Bosselut, Emma Brunskill, Erik Brynjolfsson, Shyamal Buch, Dallas Card, Rodrigo Castellon, Niladri Chatterji, Annie Chen, Kathleen Creel, Jared Quincy Davis, Dora Demszky, Chris Donahue, Moussa Doumbouya, Esin Durmus, Stefano Ermon, John Etchemendy, Kawin Ethayarajh, Li Fei-Fei, Chelsea Finn, Trevor Gale, Lauren Gillespie, Karan Goel, Noah Goodman, Shelby Grossman, Neel Guha, Tatsunori Hashimoto, Peter Henderson, John Hewitt, Daniel E. Ho, Jenny Hong, Kyle Hsu, Jing Huang, Thomas Icard, Saahil Jain, Dan Jurafsky, Pratyusha Kalluri, Siddharth Karamcheti, Geoff Keeling, Fereshte Khani, Omar Khattab, Pang Wei Koh, Mark Krass, Ranjay Krishna, Rohith Kuditipudi, Ananya Kumar, Faisal Ladhak, Mina Lee, Tony Lee, Jure Leskovec, Isabelle Levent, Xiang Lisa Li, Xuechen Li, Tengyu Ma, Ali Malik, Christopher D. Manning, Suvir Mirchandani, Eric Mitchell, Zanele Muniyikwa, Suraj Nair, Avaniika Narayan, Deepak Narayanan, Ben Newman, Allen Nie, Juan Carlos Niebles, Hamed Nilforoshan, Julian Nyarko, Giray Ogut, Laurel Orr, Isabel Papadimitriou, Joon Sung Park, Chris Piech, Eva Portelance, Christopher Potts, Aditi Raghunathan, Rob Reich, Hongyu Ren, Frieda Rong, Yusuf Roohani, Camilo Ruiz, Jack Ryan, Christopher Ré, Dorsa Sadigh, Shiori Sagawa, Keshav Santhanam, Andy Shih, Krishnan Srinivasan, Alex Tamkin, Rohan Taori, Armin W. Thomas, Florian Tramèr, Rose E. Wang, William Wang, Bohan Wu, Jiajun Wu, Yuhuai Wu, Sang Michael Xie, Michihiro Yasunaga, Jiaxuan You, Matei Zaharia, Michael Zhang, Tianyi Zhang, Xikun Zhang, Yuhui Zhang, Lucia Zheng, Kaitlyn Zhou, and Percy Liang. On the opportunities and risks of foundation models, 2021. 1
- [7] Eli Brosh, Matan Friedmann, Ilan Kadar, Lev Yitzhak Lavy, Elad Levi, Samuel Rippa, Y Lempert, Bruno Fernandez-Ruiz, Roei Herzig, and Trevor Darrell. Accurate visual localization for automotive applications. *2019 IEEE/CVF Conference on Computer Vision and Pattern Recognition Workshops (CVPRW)*, pages 1307–1316, 2019. 10
- [8] Tom B. Brown, Benjamin Mann, Nick Ryder, Melanie Subbiah, Jared Kaplan, Prafulla Dhariwal, Arvind Neelakantan, Pranav Shyam, Girish Sastry, Amanda Askell, Sandhini Agarwal, Ariel Herbert-Voss, Gretchen Krueger, Tom Henighan, Rewon Child, Aditya Ramesh, Daniel M. Ziegler, Jeffrey Wu, Clemens Winter, Christopher Hesse, Mark Chen, Eric Sigler, Mateusz Litwin, Scott Gray, Benjamin Chess, Jack Clark, Christopher Berner, Sam McCandlish, Alec Radford, Ilya Sutskever, and Dario Amodei. Language models are few-shot learners, 2020. 1
- [9] Mathilde Caron, Hugo Touvron, Ishan Misra, Hervé Jégou, Julien Mairal, Piotr Bojanowski, and Armand Joulin. Emerging properties in self-supervised vision transformers. In *Proceedings of the International Conference on Computer Vision (ICCV)*, 2021. 11
- [10] R. Chaudhry, S. Shekhar, U. Gupta, P. Maneriker, P. Bansal, and A. Joshi. Leaf-qa: Locate, encode and attend for figure question answering. In *2020 IEEE Winter Conference on Applications of Computer Vision (WACV)*, pages 3501–3510, Los Alamitos, CA, USA, mar 2020. IEEE Computer Society. 10

- [11] Guilhem Chéron, Jean-Baptiste Alayrac, Ivan Laptev, and Cordelia Schmid. A flexible model for training action localization with varying levels of supervision. In *NeurIPS*, 2018. 10
- [12] Karan Desai and Justin Johnson. Virtex: Learning visual representations from textual annotations. *2021 IEEE/CVF Conference on Computer Vision and Pattern Recognition (CVPR)*, pages 11157–11168, 2021. 10
- [13] Jacob Devlin, Ming-Wei Chang, Kenton Lee, and Kristina Toutanova. Bert: Pre-training of deep bidirectional transformers for language understanding, 2018. 1
- [14] Thomas G. Dietterich, Richard H. Lathrop, and Tomas Lozano-Perez. Solving the multiple instance problem with axis-parallel rectangles. *Artif. Intell.*, 89:31–71, 1997. 10
- [15] Xinyang Geng, Hao Liu, Lisa Lee, Dale Schuurmans, Sergey Levine, and Pieter Abbeel. Multimodal masked autoencoders learn transferable representations, 2022. 1, 9
- [16] Yulia Gryaditskaya, Mark Sypesteyn, Jan Willem Hoftijzer, Sylvia Pont, Frédo Durand, and Adrien Bousseau. Opensketch: A richly-annotated dataset of product design sketches. *ACM Trans. Graph.*, 38(6), nov 2019. 10
- [17] Geoffrey Hinton, Oriol Vinyals, Jeff Dean, et al. Distilling the knowledge in a neural network. *arXiv preprint arXiv:1503.02531*, 2(7), 2015. 2
- [18] Edward J. Hu, Yelong Shen, Phillip Wallis, Zeyuan Allen-Zhu, Yuanzhi Li, Shean Wang, and Weizhu Chen. Lora: Low-rank adaptation of large language models. *CoRR*, abs/2106.09685, 2021. 6, 9
- [19] Gabriel Ilharco, Mitchell Wortsman, Ross Wightman, Cade Gordon, Nicholas Carlini, Rohan Taori, Achal Dave, Vaishaal Shankar, Hongseok Namkoong, John Miller, Hannaneh Hajishirzi, Ali Farhadi, and Ludwig Schmidt. Openclip, 2021. 6
- [20] Maximilian Ilse, Jakub M. Tomczak, and Max Welling. Attention-based deep multiple instance learning. *ArXiv*, abs/1802.04712, 2018. 10
- [21] Achiya Jerbi, Roei Herzig, Jonathan Berant, Gal Chechik, and Amir Globerson. Learning object detection from captions via textual scene attributes. *ArXiv*, abs/2009.14558, 2020. 10
- [22] Chao Jia, Yinfei Yang, Ye Xia, Yi-Ting Chen, Zarana Parekh, Hieu Pham, Quoc V. Le, Yunhsuan Sung, Zhen Li, and Tom Duerig. Scaling up visual and vision-language representation learning with noisy text supervision. *International Conference on Machine Learning 2021*, 2021. 1, 9
- [23] K. V. Jobin, Ajoy Mondal, and C. V. Jawahar. Docfigure: A dataset for scientific document figure classification. In *2019 International Conference on Document Analysis and Recognition Workshops (ICDARW)*, volume 1, pages 74–79, 2019. 10
- [24] James D. Keeler, David E. Rumelhart, and W. Leow. Integrated segmentation and recognition of hand-printed numerals. In *NIPS*, 1990. 10
- [25] Aniruddha Kembhavi, Minjoon Seo, Dustin Schwenk, Jonghyun Choi, Ali Farhadi, and Hannaneh Hajishirzi. Are you smarter than a sixth grader? textbook question answering for multimodal machine comprehension. In *2017 IEEE Conference on Computer Vision and Pattern Recognition (CVPR)*, pages 5376–5384, 2017. 10
- [26] Wonjae Kim, Bokyoung Son, and Ildoo Kim. Vilt: Vision-and-language transformer without convolution or region supervision, 2021. 6, 7, 15
- [27] Ryan Kiros, Ruslan Salakhutdinov, and Richard S. Zemel. Unifying visual-semantic embeddings with multimodal neural language models. *ArXiv*, abs/1411.2539, 2014. 10
- [28] Michal Kucer, Diane Oyen, Juan Castorena, and Jian Wu. Deeppatent: Large scale patent drawing recognition and retrieval. *2022 IEEE/CVF Winter Conference on Applications of Computer Vision (WACV)*, pages 557–566, 2022. 10
- [29] Jieh-Sheng Lee and Jieh Hsiang. Patent claim generation by fine-tuning openai gpt-2. *ArXiv*, abs/1907.02052, 2020. 10
- [30] Thomas Leung, Yang Song, and John R. Zhang. Handling label noise in video classification via multiple instance learning. *2011 International Conference on Computer Vision*, pages 2056–2063, 2011. 10
- [31] Junnan Li, Dongxu Li, Caiming Xiong, and Steven Hoi. Blip: Bootstrapping language-image pre-training for unified vision-language understanding and generation, 2022. 1, 9

- [32] Junnan Li, Ramprasaath R. Selvaraju, Akhilesh Deepak Gotmare, Shafiq Joty, Caiming Xiong, and Steven Hoi. Align before fuse: Vision and language representation learning with momentum distillation, 2021. 1, 6, 7, 9, 15
- [33] Yangguang Li, Feng Liang, Lichen Zhao, Yufeng Cui, Wanli Ouyang, Jing Shao, Fengwei Yu, and Junjie Yan. Supervision exists everywhere: A data efficient contrastive language-image pre-training paradigm, 2021. 1, 9
- [34] Nikolaos Livathinos, Cesar Berrospi, Maksym Lysak, Viktor Kuropiatnyk, Ahmed Nassar, Andr’e C. P. L. F. de Carvalho, Michele Dolfi, Christoph Auer, Kasper Dinkla, and Peter W. J. Staar. Robust pdf document conversion using recurrent neural networks. In *AAAI*, 2021. 3
- [35] Oded Maron and Tomás Lozano-Pérez. A framework for multiple-instance learning. In M. Jordan, M. Kearns, and S. Solla, editors, *Advances in Neural Information Processing Systems*, volume 10. MIT Press, 1997. 10
- [36] Minesh Mathew, Viraj Bagal, Rubèn Tito, Dimosthenis Karatzas, Ernest Valveny, and C. V. Jawahar. Infographicvqa. In *2022 IEEE/CVF Winter Conference on Applications of Computer Vision (WACV)*, pages 2582–2591, 2022. 10
- [37] Antoine Miech, Jean-Baptiste Alayrac, Piotr Bojanowski, Ivan Laptev, and Josef Sivic. Learning from video and text via large-scale discriminative clustering. *2017 IEEE International Conference on Computer Vision (ICCV)*, pages 5267–5276, 2017. 10
- [38] Antoine Miech, Jean-Baptiste Alayrac, Lucas Smaira, Ivan Laptev, Josef Sivic, and Andrew Zisserman. End-to-end learning of visual representations from uncurated instructional videos. In *Proceedings of the IEEE/CVF Conference on Computer Vision and Pattern Recognition*, pages 9879–9889, 2020. 5, 9, 10
- [39] Antoine Miech, Dimitri Zhukov, Jean-Baptiste Alayrac, Makarand Tapaswi, Ivan Laptev, and Josef Sivic. Howto100m: Learning a text-video embedding by watching hundred million narrated video clips. *2019 IEEE/CVF International Conference on Computer Vision (ICCV)*, pages 2630–2640, 2019. 9
- [40] Ahmed Nassar, Nikolaos Livathinos, Maksym Lysak, and Peter Staar. Tableformer: Table structure understanding with transformers, 2022. 3
- [41] Alex Nichol, Prafulla Dhariwal, Aditya Ramesh, Pranav Shyam, Pamela Mishkin, Bob McGrew, Ilya Sutskever, and Mark Chen. Glide: Towards photorealistic image generation and editing with text-guided diffusion models, 2021. 1, 9
- [42] Maxime Oquab, on Bottou, Ivan Laptev, and Josef Sivic. Is object localization for free? - weakly-supervised learning with convolutional neural networks. *2015 IEEE Conference on Computer Vision and Pattern Recognition (CVPR)*, pages 685–694, 2015. 10
- [43] Birgit Pfitzmann, Christoph Auer, Michele Dolfi, Ahmed S Nassar, and Peter W J Staar. Doclaynet: A large human-annotated dataset for document-layout analysis, 2022. 3
- [44] Kader Pustu-Iren, eu, Gerrit Bruns, and Ralph Ewerth. A multimodal approach for semantic patent image retrieval. In *unknown*, 2021. 10
- [45] Gwénolé Quellec, Guy Cazuguel, Béatrice Cochener, and Mathieu Lamard. Multiple-instance learning for medical image and video analysis. *IEEE Reviews in Biomedical Engineering*, 10:213–234, 2017. 10
- [46] Alec Radford, Jong Wook Kim, Chris Hallacy, Aditya Ramesh, Gabriel Goh, Sandhini Agarwal, Girish Sastry, Amanda Askell, Pamela Mishkin, Jack Clark, Gretchen Krueger, and Ilya Sutskever. Learning transferable visual models from natural language supervision, 2021. 1, 2, 4, 6, 7, 8, 9, 10, 16, 18, 19
- [47] Colin Raffel, Noam Shazeer, Adam Roberts, Katherine Lee, Sharan Narang, Michael Matena, Yanqi Zhou, Wei Li, and Peter J. Liu. Exploring the limits of transfer learning with a unified text-to-text transformer, 2019. 1
- [48] Aditya Ramesh, Mikhail Pavlov, Gabriel Goh, Scott Gray, Chelsea Voss, Alec Radford, Mark Chen, and Ilya Sutskever. Zero-shot text-to-image generation, 2021. 1, 9
- [49] Scott Reed, Konrad Zolna, Emilio Parisotto, Sergio Gomez Colmenarejo, Alexander Novikov, Gabriel Barth-Maron, Mai Gimenez, Yury Sulsky, Jackie Kay, Jost Tobias Springenberg, Tom Eccles, Jake Bruce, Ali Razavi, Ashley Edwards, Nicolas Heess, Yutian Chen, Raia Hadsell, Oriol Vinyals, Mahyar Bordbar, and Nando de Freitas. A generalist agent, 2022. 1

- [50] Chitwan Saharia, William Chan, Saurabh Saxena, Lala Li, Jay Whang, Emily Denton, Seyed Kamyar Seyed Ghasemipour, Burcu Karagol Ayan, S. Sara Mahdavi, Rapha Gontijo Lopes, Tim Salimans, Jonathan Ho, David J Fleet, and Mohammad Norouzi. Photorealistic text-to-image diffusion models with deep language understanding, 2022. 1, 9
- [51] Christoph Schuhmann, Richard Vencu, Romain Beaumont, Robert Kaczmarczyk, Clayton Mullis, Aarush Katta, Theo Coombes, Jenia Jitsev, and Aran Komatsuzaki. Laion-400m: Open dataset of clip-filtered 400 million image-text pairs. *arXiv preprint arXiv:2111.02114*, 2021. 2
- [52] Nataliya Shapovalova, Arash Vahdat, Kevin J. Cannons, Tian Lan, and Greg Mori. Similarity constrained latent support vector machine: An application to weakly supervised action classification. In *ECCV*, 2012. 10
- [53] Amanpreet Singh, Ronghang Hu, Vedanuj Goswami, Guillaume Couairon, Wojciech Galuba, Marcus Rohrbach, and Douwe Kiela. Flava: A foundational language and vision alignment model, 2021. 1, 6, 7, 9, 15
- [54] Korsuk Sirinukunwattana, Shan e Ahmed Raza, Yee-Wah Tsang, David R. J. Snead, Ian A. Cree, and Nasir M. Rajpoot. Locality sensitive deep learning for detection and classification of nuclei in routine colon cancer histology images. *IEEE transactions on medical imaging*, 35 5:1196–1206, 2016. 10
- [55] Peter W J Staar, Michele Dolfi, Christoph Auer, and Costas Bekas. Corpus conversion service. *Proceedings of the 24th ACM SIGKDD International Conference on Knowledge Discovery and Data Mining*, Jul 2018. 3
- [56] Yi-Lin Sung, Jaemin Cho, and Mohit Bansal. VI-adapter: Parameter-efficient transfer learning for vision-and-language tasks. *2022 IEEE Conference on Computer Vision and Pattern Recognition (CVPR)*, pages 5005–5013, 2022. 6
- [57] Tristan Thrush, Ryan Jiang, Max Bartolo, Amanpreet Singh, Adina Williams, Douwe Kiela, and Candace Ross. Winoground: Probing vision and language models for visio-linguistic compositionality, 2022. 1
- [58] Naftali Tishby and Noga Zaslavsky. Deep learning and the information bottleneck principle. In *2015 IEEE information theory workshop (itw)*, pages 1–5. IEEE, 2015. 2
- [59] Ivan Vendrov, Ryan Kiros, Sanja Fidler, and Raquel Urtasun. Order-embeddings of images and language. *CoRR*, abs/1511.06361, 2016. 10
- [60] Liwei Wang, Yin Li, and Svetlana Lazebnik. Learning deep structure-preserving image-text embeddings. *2016 IEEE Conference on Computer Vision and Pattern Recognition (CVPR)*, pages 5005–5013, 2016. 10
- [61] Lewei Yao, Runhui Huang, Lu Hou, Guansong Lu, Minzhe Niu, Hang Xu, Xiaodan Liang, Zhenguo Li, Xin Jiang, and Chunjing Xu. Filip: Fine-grained interactive language-image pre-training, 2021. 1, 9
- [62] Keren Ye, Mingda Zhang, Adriana Kovashka, Wei Li, Danfeng Qin, and Jesse Berent. Cap2det: Learning to amplify weak caption supervision for object detection. *2019 IEEE/CVF International Conference on Computer Vision (ICCV)*, pages 9685–9694, 2019. 10
- [63] Jae-Chern Yoo and Tae Hee Han. Fast normalized cross-correlation. *Circuits, systems and signal processing*, 28(6):819–843, 2009. 11
- [64] Jiahui Yu, Zirui Wang, Vijay Vasudevan, Legg Yeung, Mojtaba Seyedhosseini, and Yonghui Wu. Coca: Contrastive captioners are image-text foundation models, 2022. 1, 9
- [65] Lu Yuan, Dongdong Chen, Yi-Ling Chen, Noel Codella, Xiyang Dai, Jianfeng Gao, Houdong Hu, Xuedong Huang, Boxin Li, Chunyuan Li, Ce Liu, Mengchen Liu, Zicheng Liu, Yumao Lu, Yu Shi, Lijuan Wang, Jianfeng Wang, Bin Xiao, Zhen Xiao, Jianwei Yang, Michael Zeng, Luowei Zhou, and Pengchuan Zhang. Florence: A new foundation model for computer vision, 2021. 1, 9
- [66] Xiaohua Zhai, Xiao Wang, Basil Mustafa, Andreas Steiner, Daniel Keysers, Alexander Kolesnikov, and Lucas Beyer. Lit: Zero-shot transfer with locked-image text tuning. *arXiv preprint arXiv:2111.07991*, 2021. 5, 8
- [67] Yuhao Zhang, Hang Jiang, Yasuhide Miura, Christopher D. Manning, and C. Langlotz. Contrastive learning of medical visual representations from paired images and text. *ArXiv*, abs/2010.00747, 2020. 10

- [68] Tiancheng Zhao, Tianqi Zhang, Mingwei Zhu, Haozhan Shen, Kyusong Lee, Xiaopeng Lu, and Jianwei Yin. VI-checklist: Evaluating pre-trained vision-language models with objects, attributes and relations, 2022. 16
- [69] Yi Zheng, Qitong Wang, and Margrit Betke. Semantic-based sentence recognition in images using bimodal deep learning. In *2021 IEEE International Conference on Image Processing (ICIP)*, pages 2753–2757, 2021. 3, 11
- [70] Bolei Zhou, Aditya Khosla, gata Lapedriza, Aude Oliva, and Antonio Torralba. Learning deep features for discriminative localization. *2016 IEEE Conference on Computer Vision and Pattern Recognition (CVPR)*, pages 2921–2929, 2016. 10